

Impact of alley cropping agroforestry on stocks, forms and spatial distribution of soil organic carbon: a case study in a Mediterranean context

Rémi Cardinael, Tiphaine Chevallier, Bernard Barthès, Nicolas Saby, Théophile Parent, Christian Dupraz, Martial Bernoux, Claire Chenu

► To cite this version:

Rémi Cardinael, Tiphaine Chevallier, Bernard Barthès, Nicolas Saby, Théophile Parent, et al.. Impact of alley cropping agroforestry on stocks, forms and spatial distribution of soil organic carbon: a case study in a Mediterranean context. *Geoderma*, Elsevier, 2015, 259–260, pp.288-299. 10.1016/j.geoderma.2015.06.015 . hal-01269102

HAL Id: hal-01269102

<https://hal.archives-ouvertes.fr/hal-01269102>

Submitted on 24 Jan 2020

HAL is a multi-disciplinary open access archive for the deposit and dissemination of scientific research documents, whether they are published or not. The documents may come from teaching and research institutions in France or abroad, or from public or private research centers.

L'archive ouverte pluridisciplinaire **HAL**, est destinée au dépôt et à la diffusion de documents scientifiques de niveau recherche, publiés ou non, émanant des établissements d'enseignement et de recherche français ou étrangers, des laboratoires publics ou privés.

1 **Impact of alley cropping agroforestry on stocks, forms and spatial distribution of soil**
2 **organic carbon - a case study in a Mediterranean context**

3 Rémi Cardinael^{a,d}, Tiphaine Chevallier^{a*}, Bernard G. Barthès^a, Nicolas P.A. Saby^b, Théophile
4 Parent^a, Christian Dupraz^c, Martial Bernoux^a, Claire Chenu^d

5
6 ^a IRD, UMR 210 Eco&Sols, Montpellier SupAgro, 34060 Montpellier, France

7 ^b INRA, US 1106 Infosol, F 45075, Orléans, France

8 ^c INRA, UMR 1230 System, Montpellier SupAgro, 34060 Montpellier, France

9 ^d AgroParisTech, UMR 1402 Ecosys, Avenue Lucien Brétignières, 78850 Thiverval-Grignon,
10 France

11 * Corresponding author. Tel.: +33 (0)4.99.61.21.30. E-mail address:

12 tiphaine.chevallier@ird.fr

13

14 **ABSTRACT**

15 Agroforestry systems, i.e., agroecosystems combining trees with farming practices, are of
16 particular interest as they combine the potential to increase biomass and soil carbon (C)
17 storage whilst maintaining an agricultural production. However, most present knowledge on
18 the impact of agroforestry systems on soil organic carbon (SOC) storage comes from tropical
19 systems. This study was conducted in southern France, in an 18-year-old agroforestry plot,
20 where hybrid walnuts (*Juglans regia* × *nigra* L.) are intercropped with durum wheat (*Triticum*
21 *turgidum* L. subsp. *durum*), and in an adjacent agricultural control plot, where durum wheat is
22 the sole crop. We quantified SOC stocks to 2.0 m depth and their spatial variability in relation
23 to the distance to the trees and to the tree rows. The distribution of additional SOC storage in
24 different soil particle-size fractions was also characterised. SOC accumulation rates between

25 the agroforestry and the agricultural plots were $248 \pm 31 \text{ kg C ha}^{-1} \text{ yr}^{-1}$ for an equivalent soil
26 mass (ESM) of 4000 Mg ha^{-1} (to 26-29 cm depth) and $350 \pm 41 \text{ kg C ha}^{-1} \text{ yr}^{-1}$ for an ESM of
27 15700 Mg ha^{-1} (to 93-98 cm depth). SOC stocks were higher in the tree rows where
28 herbaceous vegetation grew and where the soil was not tilled, but no effect of the distance to
29 the trees (0 to 10 m) on SOC stocks was observed. Most of additional SOC storage was found
30 in coarse organic fractions (50-200 and 200-2000 μm), which may be rather labile fractions.
31 All together our study demonstrated the potential of alley cropping agroforestry systems
32 under Mediterranean conditions to store SOC, and questioned the stability of this storage.

33

34 **Keywords:** Tree-based intercropping system, Soil mapping, Soil organic carbon storage, Soil
35 organic carbon saturation, Deep soil organic carbon stocks, Visible and near infrared
36 spectroscopy, Particle-size fractionation

37

38 1. Introduction

39 Agroforestry systems are defined as agroecosystems associating trees with farming practices
40 (Somarriba, 1992; Torquebiau, 2000). Several types of agroforestry systems can be
41 distinguished depending on the different associations of trees, crops and animals (Torquebiau,
42 2000). In temperate regions, an important part of recently established agroforestry systems are
43 alley cropping systems, where parallel tree rows are planted in crop lands, and designed to
44 allow mechanization of annual crops. Agroforestry systems are of particular interest as they
45 combine the potential to provide a variety of non-marketed ecosystem services, defined as the
46 benefits people obtain from ecosystems (Millennium Ecosystem Assessment, 2005; Power,
47 2010) whilst maintaining a high agricultural production (Clough et al., 2011). For instance,
48 agroforestry systems can contribute to water quality improvement (Bergeron et al., 2011;

49 Tully et al., 2012), biodiversity enhancement (Schroth et al., 2004; Varah et al., 2013), and
50 erosion control (Young, 1997). But agroforestry systems are also increasingly recognized as a
51 useful tool to help mitigate global warming (Pandey, 2002; Stavi and Lal, 2013; Verchot et
52 al., 2007). Trees associated to annual crops store the carbon (C) assimilated through
53 photosynthesis into their aboveground and belowground biomass. The residence time of C in
54 the harvested biomass will depend on the fate of woody products, and can reach many
55 decades especially for timber wood (Bauhus et al., 2010; Profft et al., 2009). Agroforestry
56 trees also produce organic matter (OM) inputs to the soil (Jordan, 2004; Peichl et al., 2006),
57 and could thus enhance soil organic carbon (SOC) stocks. Leaf litter and pruning residues are
58 left on the soil, whereas OM originating from root mortality and root exudates can be
59 incorporated much deeper into the soil as agroforestry trees may have a very deep rooting to
60 minimize the competition with the annual crop (Cardinael et al., 2015; Mulia and Dupraz,
61 2006). Moreover, several studies showed that root-derived C was preferentially stabilized in
62 soil compared to above ground derived C (Balesdent and Balabane, 1996; Rasse et al., 2005),
63 mainly due to physical protection of root hairs within soil aggregates (Gale et al., 2000), to
64 chemical recalcitrance of root components (Bird and Torn, 2006), or to adsorption of root
65 exudates or decomposition products on clay particles (Chenu and Plante, 2006; Oades, 1995).
66 Compared to an agricultural field, additional inputs of C from tree roots could therefore be
67 stored deep into the soil, but could also enhance decomposition of SOM, i.e., due to the
68 priming effect (Fontaine et al., 2007).

69 Although it is generally assumed that agroforestry system have the potential to increase SOC
70 stocks (Lorenz and Lal, 2014), quantitative estimates are scarce, especially for temperate
71 (Nair et al., 2010; Peichl et al., 2006; Pellerin et al., 2013; Upson and Burgess, 2013) or
72 Mediterranean (Howlett et al., 2011) agroforestry systems combining crops and tree rows.

73 Most studies concern tropical regions where agroforestry is a more widespread agricultural
74 practice (Albrecht and Kandji, 2003; Somarriba et al., 2013).

75 Moreover, as pointed out by Nair (2012), very few studies assessed the impact of agroforestry
76 trees deep in the soil (Haile et al., 2010; Howlett et al., 2011; Upson and Burgess, 2013). Most
77 of them considered SOC at depths of less than 0.5 m (Bambrick et al., 2010; Oelbermann and
78 Voroney, 2007; Oelbermann et al., 2004; Peichl et al., 2006; Sharrow and Ismail, 2004). This
79 lack of knowledge concerning deep soil is mainly due to difficulties to attain profound soil
80 depths, and to the cost of analyzing soil samples from several soil layers. Recently, new
81 methods such as visible and near infrared reflectance (VNIR) spectroscopy have been
82 developed (Brown et al., 2006; Stevens et al., 2013). They allow time- and cost-effective
83 determination of SOC concentration, in the laboratory but also in the field (Gras et al., 2014).
84 Additionally to the lack of data for deep soil, reference plots were not always available,
85 preventing from estimating the additional storage of SOC due specifically to agroforestry
86 (Howlett et al., 2011).

87 In alley cropping systems, spaces between trees in tree rows are usually covered by natural or
88 sowed herbaceous vegetation, and the soil under tree rows is usually not tilled, which may
89 favor SOC storage in soil (Virto et al., 2011). Moreover, while trees strongly affects the depth
90 and spatial distribution of OM inputs to soils (Rhoades, 1997), distribution of SOC stocks
91 close and away from trees was seldom considered. Some authors reported higher SOC stocks
92 under the tree canopy than 5 m from the tree to 1 m soil depth (Howlett et al., 2011), others
93 found that spatial distribution of SOC stocks could vary with the age of the trees (Bambrick et
94 al., 2010). Some authors reported that spatial distribution of SOC stocks to 20 cm depth was
95 not explained by the distance to the trees but by the design of the agroforestry system, tree
96 rows having higher SOC stocks than inter-rows whatever the distance to the trees (Peichl et
97 al., 2006; Upson and Burgess, 2013). To our knowledge, geostatistical methods (Webster and

98 Oliver, 2007) have never been used to describe the spatial distribution of SOC stocks in alley
99 cropping agroforestry system although they have been recognized to be very powerful to map
100 and understand spatial heterogeneity at the plot scale (Philippot et al., 2009) especially when
101 dealing with more diverse and heterogeneous systems.

102 In addition, it is not known whether additional SOC (compared to an agricultural field) due to
103 the presence of trees and tree rows, corresponds to soil fractions with a rapid turnover, such as
104 particulate organic matter (POM), or to clay and silt associated OM, likely to be stabilized in
105 soil for a longer period of time (Balesdent et al., 1998). Takimoto et al. (2008) and Howlett et
106 al. (2011) found that carbon content of coarse organic fractions was increased at different
107 depths under agroforestry systems. But, Haile et al. (2010) found that trees grown in a
108 silvopastoral system contributed to most of the SOC associated to the fine silt + clay fractions
109 to 1 m depth. The potential of a soil for SOC storage in a stable form is limited by the amount
110 of fine particles (clay + fine silt) and can be estimated by the difference between the
111 theoretical SOC saturation (Hassink, 1997) and the measured SOC saturation value for the
112 fine fraction (Angers et al., 2011; Wiesmeier et al., 2014).

113 In this study, we aimed to assess the effect of introducing rows of timber trees into arable land
114 on SOC storage. For this i) we quantified SOC stocks to a depth of 2.0 m in an agroforestry
115 plot and in an adjacent agricultural control plot, ii) we assessed the spatial distribution of SOC
116 stocks in a geostatistical framework taking into account the distance to the trees and to the
117 tree rows, iii) we studied the distribution of SOC in different soil particle-size fractions.

118 We hypothesized that SOC stocks would be higher in the agroforestry plot compared to the
119 control plot, also at depth, and that SOC stocks would decrease with increasing distance to the
120 trees at all depths. Moreover, our hypothesis was that additional SOC in the agroforestry plot
121 compared to the control plot would enrich all particle-size fractions.

122 **2. Materials and methods**

123 *2.1. Site description*

124 The experimental site was located in Prades-le-Lez, 15 km North of Montpellier,
125 France (Longitude 04°01' E, Latitude 43°43' N, elevation 54 m a.s.l.). The climate is sub-
126 humid Mediterranean with an average temperature of 14.5°C and an average annual rainfall of
127 951 mm (years 1996–2003). The soil is a silty and carbonated deep alluvial Fluvisol (IUSS
128 Working Group WRB, 2007). From 1950 to 1960, the site was a vineyard (*Vitis vinifera* L.),
129 and from 1960 to 1985 the field was occupied by an apple (*Malus* Mill.) orchard. The apple
130 tree stumps were removed in 1985. Then, durum wheat (*Triticum turgidum* L. subsp. *durum*
131 (Desf.) Husn.) was cultivated. In February 1995, a 4.6 hectare agroforestry alley-cropping
132 plot was established after the soil was ploughed to 20 cm depth, with the planting of hybrid
133 walnuts (*Juglans regia* × *nigra* cv. NG23) at 13 × 4 m spacing, with East–West tree rows
134 (Fig. 1). The remaining part of the plot (1.4 ha) was kept as a control agricultural plot. The
135 walnut trees were planted at an initial density of 200 trees ha⁻¹. They were thinned in 2004
136 down to 110 trees ha⁻¹. In the tree rows, the soil was not tilled and spontaneous herbaceous
137 vegetation grew. The cultivated inter-row was 11 m wide. Since the tree planting, the
138 agroforestry inter-row and the control plot were managed in the same way. The annual crop
139 was most of the time durum wheat, except in 1998, 2001 and 2006, when rapeseed (*Brassica*
140 *napus* L.) was cultivated, and in 2010 and 2013, when pea (*Pisum sativum* L.) was cultivated.
141 The durum wheat crop was fertilized as a conventional crop (120 kg N ha⁻¹ yr⁻¹), and the soil
142 was ploughed annually to 20 cm depth, before durum wheat was sown.

143

144

145



146

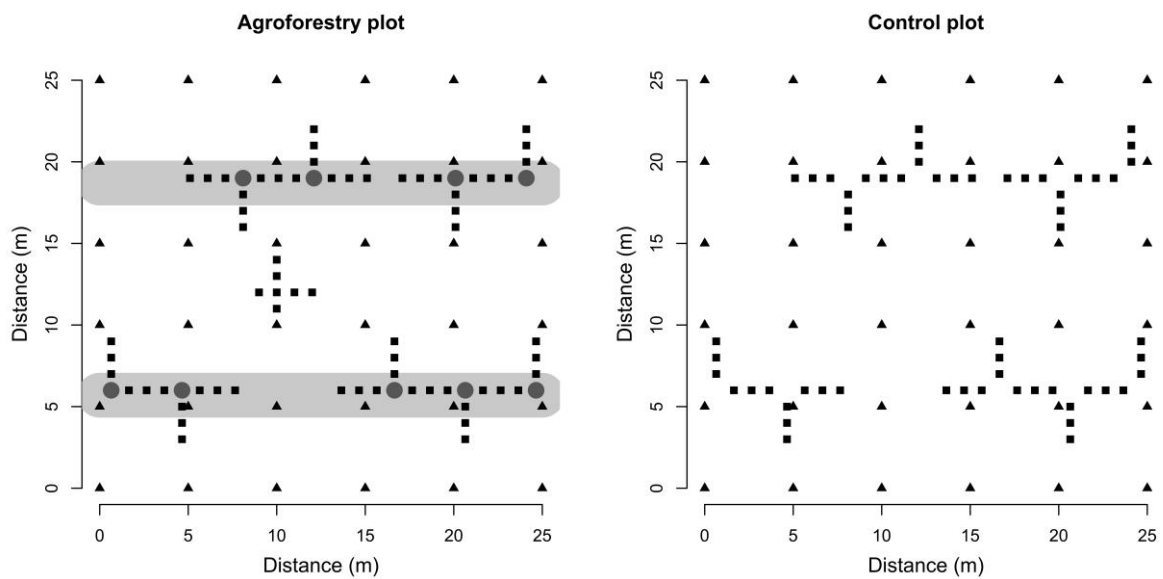
147 Figure 1. Hybrid walnut-durum wheat agroforestry system. Left panel: in November 2013;
148 Right panel: in June 2014.

149

150 *2.2. Soil core sampling*

151 The experimental site was not designed as traditional agronomical experiments with blocks
152 and replicates, but with two large adjacent plots. First, soil texture was analyzed for 24
153 profiles down to 2 m soil depth, following a random sampling design within the two plots. In
154 May 2013, a sub-plot of 625 m² was sampled in both plots, following an intensive sampling
155 scheme (Fig. 2). In the agroforestry plot, this sub-plot included two tree rows, two inter-rows
156 and nine walnut trees. Walnut trees had a mean height of 11.21 ± 0.65 m, a mean height of
157 merchantable timber of 4.49 ± 0.39 m and a mean diameter at breast height of 25.54 ± 1.36
158 cm. Soil cores (n=36) were sampled on a regular grid, every 5 m (Fig. 2). Around each tree, a
159 soil core was collected at 1 m, 2 m and 3 m distance from the tree (n=57), in the tree row and
160 perpendicular to the tree row. Seven soil cores were sampled additionally in the middle of the
161 inter-row to study short scale (1 m distance) spatial heterogeneity of SOC stocks far from the
162 trees (Fig. 2). The same sampling scheme was followed in the control plot without these seven
163 additional soil cores. Thus, 100 soil cores were sampled in the agroforestry sub-plot (40 in

164 tree rows, 60 in inter-rows) and 93 in the agricultural sub-plot (Fig. 2). All cores were
 165 sampled down to 2 m depth using a motor-driven micro caterpillar driller (8.5-cm diameter
 166 and 1-m long soil probe). The soil probe was successively pushed two times into the soil, to
 167 get 0-1 m and 1-2 m cores at each sampling point. Each soil core was then cut into ten
 168 segments, corresponding to the following depth increments: 0-10, 10-30, 30-50, 50-70, 70-
 169 100, 100-120, 120-140, 140-160, 160-180, and 180-200 cm.



170
 171 Figure 2. Description of the intensive sampling scheme in the agroforestry and in the control
 172 sub-plots. Circles represent hybrid walnuts, the grey strips represents the tree rows,
 173 triangles are for soil cores on the regular grid (every 5 m), squares are for soil cores
 174 on transects (every 1 m).

175
 176 *2.3. Use of field visible and near infrared spectroscopy to predict SOC*

177 As core surface had been smoothed by the soil probe, each segment was refreshed with
 178 a knife before being scanned, in order to provide a plane but un-smoothed surface. Then, four
 179 VNIR spectra (from 350 to 2500 nm at 1 nm increment) were acquired in the field at different

180 places of each segment, using a portable spectrophotometer ASD LabSpec 2500 (Analytical
181 Spectral Devices, Boulder, CO, USA), and were then averaged. Reflectance spectra were
182 recorded as absorbance, which is the logarithm of the inverse of reflectance. The whole
183 spectrum population was composed of 1908 mean spectra (i.e. 193 cores with 10 sub-cores
184 per core but a few samples were lost due to mechanical problems). In topsoil (0-30 cm), the
185 soil was dry and crumbled whereas in deeper soil horizons, it was moister and had higher
186 cohesion. Thus, two different predictive models were built: one for topsoil samples, the other
187 for subsoil (30-200 cm) samples. The “topsoil model” for predicting SOC was built using the
188 116 most representative topsoil samples, out of 380 samples, and the “subsoil model”, using
189 the 142 most representative subsoil samples, out of 1488 samples. The procedure to select the
190 most representative samples is presented below. The 0-10 cm soil layer from the tree rows (40
191 samples) was not used for the topsoil model as it contained abundant plant debris < 2 mm
192 (roots, leaves, etc.) and a PCA revealed that these VNIR spectra were different from the
193 whole spectra population. SOC concentration of these samples was therefore determined with
194 a CHN elemental analyzer, and, thus, not predicted by VNIR. The SOC concentration of the
195 258 samples selected for building the VNIR prediction models was also analyzed using a
196 CHN elemental analyzer.

197

198 *2.4. VNIR spectra analysis and construction of predictive models*

199 VNIR spectra analysis was conducted on topsoil and subsoil samples separately, using
200 the WinISI 4 software (Foss NIRSystems/ Tecator Infracore International, LLC, Silver Spring,
201 MD, USA) and R software version 3.1.1 (R Development Core Team, 2013). The most
202 representative samples, from a spectral viewpoint, were selected using the Kennard-Stone
203 algorithm, which is based on distance calculation between sample spectra in the principal

204 component space (Kennard and Stone, 1969). For the topsoil model, the calibration subset
205 included 104 samples (90%) selected as the most representative spectrally, and the validation
206 subset 12 samples (10%). For the subsoil model, the calibration subset included 128 samples
207 (90%), and the validation subset 14 samples. Fitting the spectra to the SOC concentrations
208 determined with a CHN elemental analyzer was performed using partial least squares
209 regression (PLSR; Martens and Naes, 1989). We tested common spectrum preprocessing
210 techniques including first and second derivatives, de-trending, standard normal variate
211 transformation and multiplicative scatter correction, but the best models were obtained when
212 no pre-treatment was applied on the spectra (data not shown). Then cross-validation was
213 performed within the calibration subset, using groups that were randomly selected (10
214 groups), in order to build the model used for making predictions on the samples not analyzed
215 in the laboratory. No outlier was removed. The number of components (latent variables) that
216 minimized the standard error of cross-validation (SECV) was retained for the PLSR. The
217 performance of the models was assessed on the validation subsets using the coefficient of
218 determination (R^2) and the standard error of prediction (SEP) between predicted and measured
219 values, and also the ratio of standard deviation to SEP, denoted RPD, and the RPIQ, which is
220 the ratio of performance to IQ (interquartile distance), i.e. $IQ/SEP = (Q3 - Q1)/SEP$, where
221 $Q1$ is the 25th percentile and $Q3$ is the 75th percentile (Bellon-Maurel et al., 2010). Then all
222 sub-set samples (i.e., calibration and validation samples) were used to build models that were
223 applied on the samples not analyzed in the laboratory. The performance of these models was
224 also assessed according to R^2 , SECV, RPD and RPIQ.

225

226

227

228 Table 1. External validation and prediction model results for soil organic carbon. N: numbers of samples; SD: standard deviation (mean and
 229 standard deviation of the conventional determinations); R²: coefficient of determination; RPD is the ratio of performance to deviation,
 230 i.e. the ratio of SD to SEP or SECV. RPIQ is the ratio of performance to IQ (interquartile distance), i.e. IQ/SEP (or SECV) = (Q3 -
 231 Q1)/SEP (or SECV).

Topsoil														
External validation on 10% samples after calibration using 90% samples								Prediction model using 100% samples (10-group cross-validation)						
N	Mean mg g ⁻¹	SD mg g ⁻¹	SEP mg g ⁻¹	Bias mg g ⁻¹	R ²	RPD	RPIQ	N	Mean mg g ⁻¹	SD mg g ⁻¹	SECV mg g ⁻¹	R ²	RPD	RPIQ
12	9.71	2.09	1.04	-0.59	0.78	1.75	2.60	116	9.18	1.99	1.20	0.63	1.66	4.35

Subsoil														
External validation on 10% samples after calibration using 90% samples								Prediction model using 100% samples (10-group cross-validation)						
N	Mean mg g ⁻¹	SD mg g ⁻¹	SEP mg g ⁻¹	Bias mg g ⁻¹	R ²	RPD	RPIQ	N	Mean mg g ⁻¹	SD mg g ⁻¹	SECV mg g ⁻¹	R ²	RPD	RPIQ
14	6.19	1.80	0.83	0.01	0.74	2.03	3.03	142	6.06	1.86	0.77	0.83	2.40	4.85

232

233

234 Subsoil models performed better than topsoil models (Table 1, Fig. S1). In external
235 validation, RPD was higher than 2 for the subsoil, which has been considered a threshold for
236 accurate NIRS prediction of soil properties in the laboratory (Chang et al., 2001). This RPD
237 threshold was not achieved for the topsoil model, but SOC concentrations were predicted for
238 less than 60% of topsoil samples, the rest was directly analyzed with a CHN elemental
239 analyzer. It is worth noting that cross-validation on the whole set (for making prediction on
240 the samples not analyzed in the lab) yielded better results than external validation (on 10% of
241 analyzed samples) in the subsoil, but the opposite was observed in the topsoil.

242

243 *2.5. Bulk densities determination*

244 Each segment was weighed in the field to determine its humid mass. Following this
245 step, each segment was crumbled and homogenized, and a representative sub-sample of about
246 300 g was sampled. Sub-samples were sieved at 2 mm to separate coarse fragments such as
247 stones and living roots. Coarse fragments represented less than 1% of each soil mass and were
248 considered as negligible. Moisture contents were determined for 23 soil cores (i.e. 230
249 samples) after 48 h drying at 105°C, and were used to calculate the dry mass of all samples.
250 Bulk density (BD) was determined for each sample by dividing the dry mass of soil by its
251 volume in the soil corer tube.

252

253 *2.6. Reference analysis measurements*

254 After air drying, soil samples were oven dried at 40°C for 48 hours, sieved at 2 mm,
255 and ball milled until they passed a 200 µm mesh sieve. Carbonates were removed by acid
256 fumigation, following Harris et al., (2001). For this, 30 mg of soil was placed in open Ag-foil

257 capsules. The capsules were then placed in the wells of a microtiter plate and 50 μ L of
258 demineralized water was added in each capsule. The microtiter plate was then placed in a
259 vacuum desiccator with a beaker filled with 100 mL of concentrated HCl (37%). The samples
260 were exposed to HCl vapors for 8 hours, and were then dried at 60°C for 48 hours. Capsules
261 were then closed in a bigger tin capsule. Decarbonated samples were analyzed for organic
262 carbon concentration with a CHN elemental analyzer (Carlo Erba NA 2000, Milan, Italy).
263 Isotopic measurements were performed on a few samples to check that decarbonation was
264 well performed ($\delta^{13}\text{C OM} = -25 \text{ ‰}$).

265

266 *2.7. Soil organic carbon stock calculation*

267 In most studies comparing SOC stocks between treatments or over time periods, SOC
268 stocks have been quantified to a fixed depth as the product of soil bulk density, depth and
269 SOC concentration. However, if soil bulk density differs between the treatments being
270 compared, the fixed-depth method has been shown to introduce errors (Ellert et al., 2002). A
271 more accurate method is to use an equivalent soil mass (ESM) (Ellert and Bettany, 1995). We
272 defined a reference soil mass profile that was used as the basis for comparison, based on the
273 lowest soil mass observed at each sampling depth and location. For this reference, soil mass
274 layers (0-1000, 1000-4000, 4000-7300, 7300-10700, 10700-15700, 15700-18700, 18700-
275 21900, 21900-25100, 25100-28300, 28300-31500 Mg ha^{-1}) corresponded roughly to soil
276 depth layers (0–10, 10–30, 30–50, 50-70, 70-100, 100-120, 120-140, 140-160, 160-180, 180-
277 200 cm, respectively). For the different treatments (control, tree row, inter-row), SOC stocks
278 were calculated on this basis, soil mass was the same, whereas depth layer varied (Table 2).
279 The effect of the ESM correction can be seen in Table S1. SOC stocks in the agroforestry plot
280 were calculated with tree rows representing 16% of the plot surface area and inter-rows 84%:

281
$$\text{SOC stock}_{\text{Agroforestry}} = 0.16 \times \text{SOC stock}_{\text{Tree row}} + 0.84 \times \text{SOC stock}_{\text{Inter row}} \quad (1)$$

282 We defined delta SOC stock as the difference between SOC stock in the agroforestry plot and
283 in the control plot:

284
$$\Delta \text{SOC stock} = \text{SOC stock}_{\text{Agroforestry}} - \text{SOC stock}_{\text{Control}} \quad (2)$$

285 All SOC stocks were expressed in Mg C ha⁻¹. SOC accumulation rates (kg C ha⁻¹ yr⁻¹) were
286 calculated by dividing delta stocks by the number of years since the tree planting (18 years):

287
$$\text{SOC accumulation rate} = \frac{\Delta \text{SOC stock}}{18} \times 1000 \quad (3)$$

288 *2.8. Particle-size fractionation*

289 Particle-size fractionation was performed for five soil cores from the inter-rows, five from the
290 tree rows and six from the control plot, and at four depths: 0-10, 10-30, 70-100 and 160-
291 180 cm. Thus, 64 soil samples were fractionated, as described in Balesdent et al. (1998) and
292 Gavinelli et al. (1995). Briefly, 20 g of 2-mm sieved samples were soaked overnight at 4°C in
293 300 mL of deionized water, with 10 mL of sodium metaphosphate (HMP, 50 g L⁻¹). Samples
294 were then shaken 2 h with 10 glass balls in a rotary shaker, at 43 rpm. The soil suspension
295 was wet-sieved through 200-µm and 50-µm sieves, successively. The fractions remaining on
296 the sieves were density-separated into organic fractions, floating in water, and remaining
297 mineral fractions. The 0-50 µm suspension was ultrasonicated during 10 min with a probe-
298 type ultrasound generating unit (Fisher Bioblock Scientific, Illkirch, France) having a power
299 output of 600 watts and working in 0.7:0.3 operating/interruption intervals. This 0-50 µm
300 suspension was then sieved through a 20-µm sieve. The resulting 0-20 µm suspension was
301 transferred to 1-L glass cylinders, which were then shaken by hand and 50 mL of the
302 suspension were withdrawn immediately after. They constituted an aliquot of the entire 0-20
303 µm fraction. After a settling time of 8 h approximately, a second aliquot of 50 mL was

304 removed by siphoning the upper 10 cm of the suspension left after the first sampling. This
305 represented an aliquot of the 0-2 μm fraction. A third aliquot was also collected in the upper
306 10 cm, and centrifuged two times 35 min, at 4000 rpm. This aliquot was then filtered at 2 μm
307 to get the hydrosoluble fraction. Fractions were then dried at 40°C, finely ground,
308 decarbonated and analyzed with a CHN elemental analyzer. A binocular microscope was used
309 to check if separation of coarse mineral fractions and of light organic coarse fractions (200-
310 2000 and 50-200 μm) was well done. No pyrogenic particles were observed. Organic carbon
311 contents of coarse mineral fractions were then assumed to be 0 mg C g⁻¹. A sub-sample of
312 each of the 64 selected samples was used to perform a classical textural analysis after
313 destruction of organic matter. These texture analyses were used to evaluate the quality of the
314 dispersion for soil particle size fractionation.

315

316 2.9. Calculation of SOC saturation

317 The theoretical value of SOC saturation was calculated according to the equation proposed by
318 (Hassink, 1997):

$$319 \quad SOC_{sat-pot} = 4.09 + 0.37 \times \text{particles} < 20 \mu\text{m} \quad (4)$$

320 where $SOC_{sat-pot}$ is the potential SOC saturation (mg C g⁻¹) and where particles < 20 μm
321 represents the proportion of fine soil particles <20 μm (%).

322 To calculate the SOC saturation deficit (Angers et al., 2011; Wiesmeier et al., 2014), the
323 estimated current SOC concentrations of the fine fraction were subtracted from the potential
324 SOC saturation:

$$325 \quad SOC_{sat-def} = SOC_{sat-pot} - SOC_{cur} \quad (5)$$

326 where $SOC_{sat-def}$ is the SOC saturation deficit ($mg\ C\ g^{-1}$) and SOC_{cur} is the current mean SOC
 327 concentration of the fine fraction $<20\ \mu m$ ($mg\ C\ g^{-1}$). The total amount of the SOC storage
 328 potential ($SOC_{stor-pot}$, $Mg\ C\ ha^{-1}$) was calculated multiplying $SOC_{sat-def}$ by soil bulk density and
 329 soil layer thickness.

330 These calculations were performed for the four depths where particle-size fractionation was
 331 done (0-10, 10-30, 70-100 and 160-180 cm). But as the equation proposed by (Hassink, 1997)
 332 was calibrated for topsoil layers, calculations for deep soil layers are only indicative.

333

334 2.10. Statistical analyses

335 The observed variability in a soil property Z such as SOC concentration results from complex
 336 processes operating over various spatial scales. A simple but useful statistical model for Z at a
 337 set of observations that could be spatially located, $\mathbf{s}_i = \{s_1, s_2, \dots, s_q\}$ is

$$338 \quad Z(\mathbf{s}_i) = \mu(\mathbf{s}_i) + \varepsilon(\mathbf{s}_i) \quad (6)$$

339 where $\mu(\mathbf{s}_i)$ is a deterministic component and $\varepsilon(\mathbf{s}_i)$ is a correlated random component that
 340 can include a pure noise random one. A soil property can be correlated with other
 341 environmental variables such as, in this work, the distance to the closest tree. This can be
 342 represented in Equation 6 by assuming that $\mu(\mathbf{s}_i)$ comprises an additive combination of one
 343 or more fixed effect:

$$344 \quad \mu(\mathbf{s}_i) = \beta_0 + \sum_{j=1}^q \beta_j x_j(\mathbf{s}_i) \quad (7)$$

345 where x_j ($j = 1, 2, \dots, q$) are q auxiliary variables and β_0, \dots, β_q are the associated fixed
 346 effects. This model is referred as a Mixed Effects Model which offers a flexible framework by
 347 which to model the sources of variation and correlation that arise from grouped data (Lark et

348 al., 2006; Pinheiro and Bates, 2000). In this work, we fitted two different linear mixed models
349 (LMM).

350 We first fitted a LMM using the whole set of the bulk densities, SOC concentrations, and
351 SOC stocks observations at the different depths. We used the *nlme* package (Pinheiro et al.,
352 2013). Soil core ID was considered as a random effect to take into account a sample effect.
353 These soil properties were then compared by depth and per location (control, tree row, inter-
354 row). An ANOVA was performed on these models. We then used the *multcomp* package
355 (Hothorn et al., 2008) to perform a post hoc analysis and determine which means differed
356 significantly between the control, tree rows and inter-rows, using the Tukey-Kramer test,
357 designed for unbalanced data. To study spatial influence on SOC stocks, “distance to the
358 closest tree” was added to the LMM model, and an ANOVA was performed.

359 Secondly, we fitted a LMM in a geostatistical framework using the cumulated SOC stock
360 observations for 3 depths (0-30 cm, 0-100 cm and 0-200 cm). In a spatial context, the random
361 effects of the LMM describe spatially-correlated random variation. The LMM model is then
362 parameterized by a global vector, called Θ , of model parameters which include the parameters
363 of the covariance function and the fixed effects coefficients. These can be fitted to the data by
364 a likelihood method. Lark et al. (2006) described how the maximum likelihood estimator is
365 biased in the presence of fixed effects and suggested that the restricted maximum likelihood
366 estimator (REML) should be applied. Following Villanneau et al., (2011) we have tested the
367 assumption that the random effects are spatially correlated by comparing the quality of the
368 model-fit for spatially correlated and spatially independent models (usually called pure nugget
369 model). Webster and McBratney, (1989) suggested that the Akaike information criterion
370 (AIC, Akaike, 1974) should be used to compare different spatially correlated models. Once
371 the parameters of the LMM have been fitted, they may be plugged into the best linear
372 unbiased predictor to form the empirical best linear unbiased predictor (E-BLUP) of the

373 property at unsampled sites (Lark et al., 2006). The error variance of the E-BLUP can also be
374 computed at any unsampled site. For this, the value of fixed effects covariates must be known
375 at each prediction site. We therefore calculated several grids of the fixed effects with a 25 cm
376 cell size. The use of any model of spatial variation implies that assumptions have been made
377 about the type of variation the data exhibit. Once the model has been fitted, cross-validation
378 can be used to confirm that these assumptions are reasonable and that the spatial model
379 appropriately describes the variation. We therefore computed a ‘leave-one-out cross-
380 validation’. For each sampling location, \mathbf{s}_i ($i = 1, 2, \dots, q$), the value of the property at \mathbf{s}_i was
381 predicted by the E-BLUP upon the vector of observations excluding $Z(\mathbf{s}_i)$, in order to
382 compute the standardized squared prediction error (SSPE: the squared difference between the
383 E-BLUP and the observed value divided by the computed prediction error variance (PEV)).
384 Under an assumption of normal prediction errors, the expected mean SSPE is 1.0 if the PEVs
385 are reliable (which requires an appropriate variogram model), and the expected median SSPE
386 is 0.455. The spatial analysis package *GeoR* (Ribeiro and Diggle, 2001) was used for REML
387 fitting and kriging.

388 Finally, a Kruskal-Wallis test (Kruskal and Wallis, 1952) was performed to analyze SOC
389 concentration in soil fractions per depth and per location (5 or 6 replicates). This test was
390 followed by a post hoc analysis using Dunn’s test (Dunn, 1964) with a Bonferroni correction
391 (p-value=0.017).

392 All the statistical analyses were performed using R software version 3.1.1 (R Development
393 Core Team, 2013), at a significance level of <0.05.

394

395

396

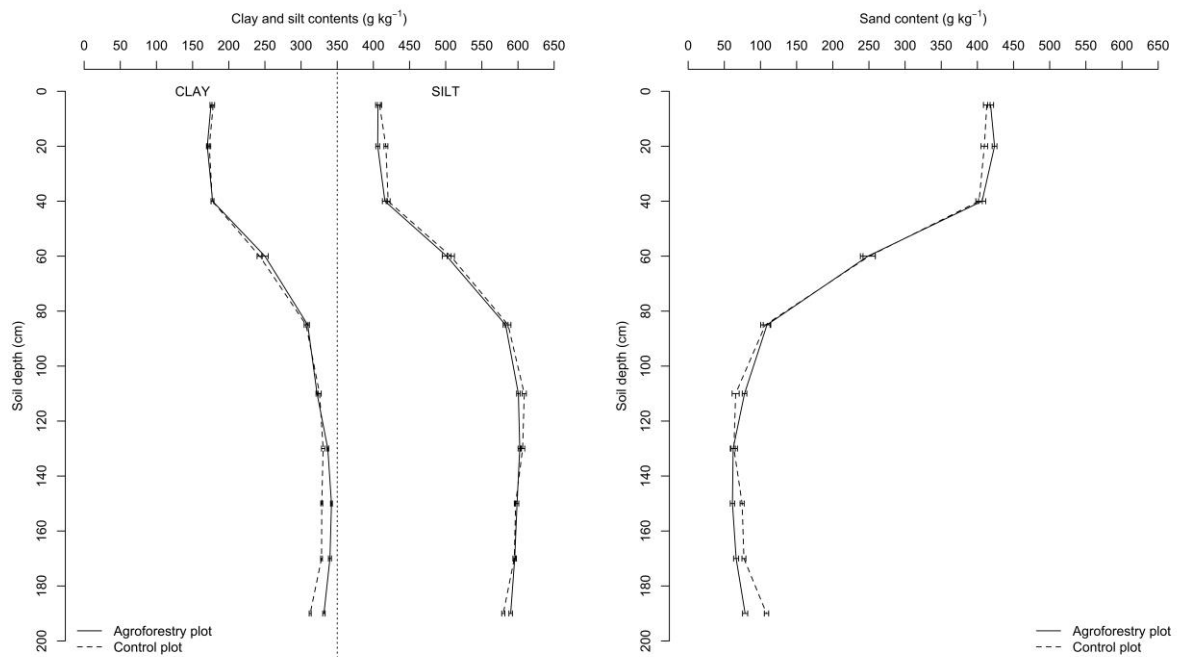
397 Table 2. Soil organic carbon stocks (Mg C ha⁻¹) and SOC accumulation rates (kg C ha⁻¹ yr⁻¹). Associated errors are standard errors (40 replicates
 398 for the tree-row, 60 replicates for the inter-row, and 93 replicates for the control plot). ESM = Equivalent Soil Mass. Significantly (p-
 399 value<0.05) different SOC stocks are followed by different letters.

Cumulated ESM (Mg ha ⁻¹)	Cumulated calculated depth to ESM (cm)			Cumulated SOC stocks (Mg C ha ⁻¹)				Δ SOC stocks (Mg C ha ⁻¹)	SOC accumulation rates (kg C ha ⁻¹ yr ⁻¹)	
	Tree-row	Inter-row	Control	Tree-row	Inter-row	Agroforestry	Control	Δ (Agroforestry – Control)	Agroforestry vs Control	Inter-row vs Control
1000	0-9	0-8	0-7	21.6 ± 1.0 a	9.8 ± 0.4 c	11.7 ± 0.3 b	9.3 ± 0.1 c	2.3 ± 0.4	129 ± 20	24 ± 21
4000	0-29	0-27	0-26	52.8 ± 1.4 a	37.9 ± 0.6 c	40.3 ± 0.5 b	35.8 ± 0.2 d	4.5 ± 0.6	248 ± 31	115 ± 33
7300	0-49	0-47	0-45	77.1 ± 1.5 a	62.0 ± 0.7 c	64.4 ± 0.6 b	59.4 ± 0.2 d	5.0 ± 0.6	276 ± 36	141 ± 39
10700	0-69	0-66	0-64	98.1 ± 1.5 a	82.4 ± 0.7 c	84.9 ± 0.6 b	79.7 ± 0.3 d	5.1 ± 0.7	286 ± 39	147 ± 43
15700	0-98	0-95	0-93	130.4 ± 1.5 a	113.7 ± 0.7 c	116.4 ± 0.7 b	110.1 ± 0.3 d	6.3 ± 0.7	350 ± 41	202 ± 45
18700	0-118	0-115	0-112	150.3 ± 1.5 a	133.1 ± 0.8 c	135.9 ± 0.7 b	129.3 ± 0.4 d	6.5 ± 0.8	363 ± 43	210 ± 46
21900	0-137	0-134	0-131	170.9 ± 1.5 a	152.8 ± 0.8 c	155.7 ± 0.7 b	149.5 ± 0.4 c	6.2 ± 0.8	345 ± 44	185 ± 48
25100	0-157	0-154	0-150	191.0 ± 1.6 a	172.4 ± 0.8 c	175.4 ± 0.7 b	169.9 ± 0.4 c	5.5 ± 0.8	306 ± 45	140 ± 49
28300	0-176	0-173	0-170	209.5 ± 1.6 a	190.5 ± 0.8 c	193.5 ± 0.7 b	189.3 ± 0.4 c	4.3 ± 0.8	238 ± 47	69 ± 51
31500	0-196	0-193	0-189	226.1 ± 1.6 a	206.0 ± 0.84 c	209.2 ± 0.7 b	205.9 ± 0.4 c	3.3 ± 0.9	183 ± 48	5 ± 53

400 **3. Results**

401 *3.1. Changes in soil texture with depth*

402 Clay, silt and sand profiles were very similar at both plots (Fig. 3). Soil texture was
403 homogeneous in the first 50 cm. Clay and silt contents linearly increased till 100 cm soil
404 depth to reach about 325 g kg⁻¹ and 575 g kg⁻¹ respectively, while sand content decreased. Soil
405 texture did not change between 100 and 200 cm soil depth. Below 140 cm depth, clay and
406 sand content were significantly different (F=71.31, P<0.001) in both plots, but the maximum
407 difference was less than 20 g kg⁻¹.



408

409 Figure 3. Changes in soil texture with depth in the control plot and in the agroforestry plot.

410 Error bars represent standard errors (n=100 in the agroforestry, n=93 in the control).

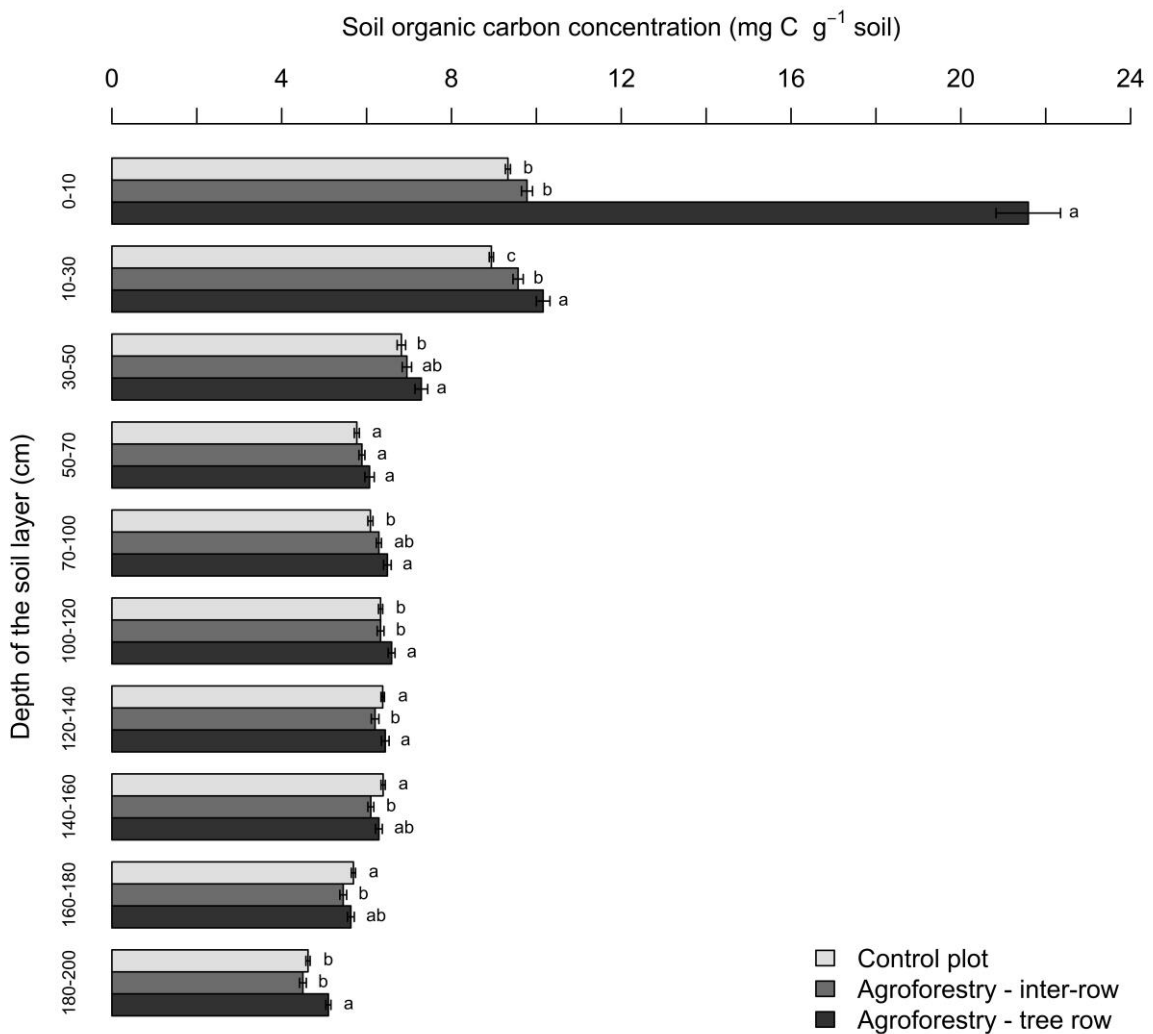
411

412

413

414 3.2. Soil bulk densities

415 Soil bulk densities were significantly higher in the control plot than in the tree row at all
 416 depths except for 30-50 and 140-160 cm, and higher than in the inter-row, except for 10-30
 417 and below 140 cm depth (Table 3). In the agroforestry system, soil bulk densities were higher
 418 in the inter-row than in the tree row for 0-10 and 10-30 cm.



419
 420 Figure 4. Soil organic carbon concentration (mg C g⁻¹ soil) of soil layers to 2-m depth in the
 421 control plot and in the agroforestry plot. Error bars represent standard errors (n=100
 422 in the agroforestry, n=93 in the control). Significantly (p-value<0.05) different SOC
 423 concentrations per depth are followed by different letters.

424 Table 3. Mean soil bulk densities (g cm^{-3}). For a given depth, means followed by the same letters do not differ significantly at $p = 0.05$.

425 Associated errors are standard errors (40 replicates for the tree-row, 60 replicates for the inter-row, and 93 replicates for the control plot).

426

Depth (cm)	Agroforestry – tree row	Agroforestry – inter-row	Control plot
0-10	1.10 ± 0.02 c	1.23 ± 0.03 b	1.41 ± 0.01 a
10-30	1.49 ± 0.01 b	1.60 ± 0.02 a	1.61 ± 0.00 a
30-50	1.71 ± 0.01 ab	1.67 ± 0.02 b	1.73 ± 0.00 a
50-70	1.73 ± 0.01 c	1.77 ± 0.01 b	1.80 ± 0.00 a
70-100	1.68 ± 0.00 c	1.71 ± 0.00 b	1.74 ± 0.00 a
100-120	1.55 ± 0.01 b	1.55 ± 0.01 b	1.61 ± 0.00 a
120-140	1.63 ± 0.00 b	1.64 ± 0.01 b	1.65 ± 0.00 a
140-160	1.64 ± 0.00 a	1.64 ± 0.01 a	1.65 ± 0.00 a
160-180	1.62 ± 0.01 b	1.65 ± 0.01 a	1.65 ± 0.00 a
180-200	1.64 ± 0.00 b	1.65 ± 0.00 a	1.65 ± 0.00 a

427

428

429

430

431

432

433

434

435 *3.3. Soil organic carbon concentrations*

436 An ANOVA performed on the LMM model revealed that soil depth (F-value=270, $P<0.0001$)
437 and location, i.e., tree row vs. inter-row (F-value=171, $P<0.0001$), were the only variables
438 affecting significantly SOC concentrations. Distance to the closest tree had no significant
439 effect (F-value=1.3, $P=0.28$). As shown in Fig. 4, for 0-10 cm, SOC concentration doubled in
440 the tree row (21.6 ± 0.8 mg C g⁻¹) compared to the inter-row (9.8 ± 0.1 mg C g⁻¹) and to the
441 control (9.3 ± 0.1 mg C g⁻¹), whereas the latter two were not significantly different. SOC
442 concentration was significantly higher in the tree row than in the control plot to 120 cm soil
443 depth, except in the 50-70 cm soil layer where no difference was observed. SOC
444 concentration was significantly higher in the tree row than in the inter-row to 30 cm soil
445 depth.

446

447 *3.4. Soil organic carbon stocks*

448 Fig. 5 represents SOC stocks in the agroforestry plot as a function of soil depth, location and
449 distance to the closest tree. For a given depth and distance to the closest tree, variability of
450 SOC stocks was high, and there was no effect of the distance to the closest tree on SOC stocks
451 (Fig. 5). An ANOVA performed on the LMM model confirmed that SOC stocks were
452 significantly influenced by soil depth (F-value=483, $P<0.0001$) and location, i.e., tree row vs.
453 inter-row (F-value=66, $P<0.0001$), but not by the distance to the closest tree (F-value=1.5,
454 $P=0.22$).

455 For an equivalent soil mass (ESM) of 4000 Mg ha⁻¹ (to 26-29 cm depth), SOC stocks were
456 significantly higher in the tree row than in the inter row and in the control (Table 2). For an
457 ESM of 31500 Mg ha⁻¹ (to 189-196 cm depth), SOC stocks were about 20 Mg C ha⁻¹ higher in
458 the tree rows compared to the inter-rows or to the control. Cumulated SOC stocks were

459 significantly higher in the inter-row than in the control plot to an ESM of 18700 Mg ha⁻¹ (to
460 112-115 cm depth), except for an ESM of 1000 Mg ha⁻¹ where not difference was found
461 (Table 2).

462 At the plot scale, cumulated SOC stocks in the agroforestry plot were significantly higher than
463 in the control plot at all depths (Table 2). For an ESM of 4000 Mg ha⁻¹ (to 26-29 cm depth),
464 SOC stocks were 40.3 ± 0.5 Mg C ha⁻¹ and 35.8 ± 0.2 Mg C ha⁻¹ in the agroforestry and in the
465 control, respectively. For a soil mass of 15700 Mg ha⁻¹ (to 93-98 cm depth), Δ SOC stock
466 between the agroforestry and the control was 6.3 ± 0.7 Mg C ha⁻¹. This difference was much
467 lower without the ESM correction (Table S1).

468

469 *3.5. Soil organic carbon accumulation rates*

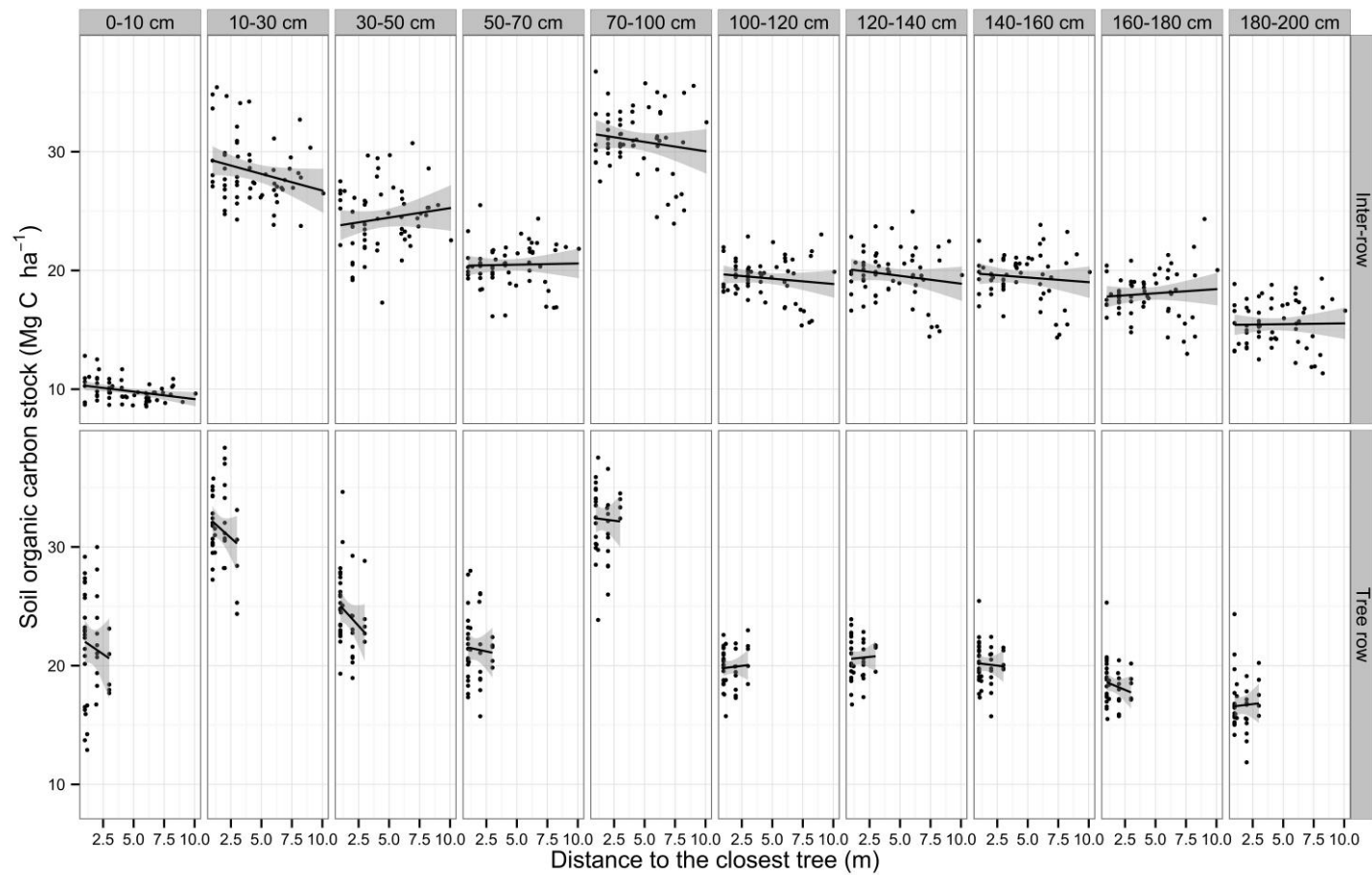
470 Compared to the control, inter-rows accumulated 115 ± 33 kg C ha⁻¹ yr⁻¹ for an ESM of 4000
471 Mg ha⁻¹ (26-29 cm) (Table 2), and 202 ± 45 kg C ha⁻¹ yr⁻¹ for an ESM of 15700 Mg ha⁻¹ (93-
472 98 cm). SOC accumulation rates in the agroforestry plot compared to the control were 248 ±
473 31 kg C ha⁻¹ yr⁻¹ for an ESM of 4000 Mg ha⁻¹, 350 ± 41 kg C ha⁻¹ yr⁻¹ an ESM of 15700 Mg
474 ha⁻¹, and 183 ± 48 kg C ha⁻¹ yr⁻¹ an ESM of 31500 Mg ha⁻¹ (Table 2). The additional SOC
475 storage rates for 0-10 cm and 10-30 cm were respectively explained at 80% and 60% by the
476 tree rows.

477

478

479

480



481

482 Figure 5. Soil organic carbon stocks (Mg C ha⁻¹) in the agroforestry plot as a function of depth, location (tree row vs. inter-row) and
 483 the closest tree. The lines represent the regression lines fitted using soil samples per investigated depth. The gray shades display the
 484 prediction confidence interval at the 0.95 level.

485 Table 4. Summary of selected models fitted to the data on cumulated soil organic carbon stocks at 3 depths (0-30 cm, 0-100 cm and 0-200 cm)
 486 for the 2 plots, and cross validation. SSPE, standardized squared prediction errors; ME, mean error (Mg C ha⁻¹); RMSQE, root mean
 487 squared error (Mg C ha⁻¹); AIC, AIC of the spatially correlated model; AIC.ns, AIC of the non-spatially correlated model; β_0 and β_1 the
 488 fixed effects (Mg C ha⁻¹). Bold characters represent the smallest AIC for each depth. The medians and the mean of the cross validation
 489 statistics are within the 95% confidence interval.

	Depth (cm)	Mean SSPE	Median SSPE	ME	RMQSE	AIC	AIC.ns	β_0	β_1	Nugget	Sill	Range	Nugget to Sill ratio
Agroforestry	0-30	0.99	0.36	-0.004	20.7	585	583	38.1	14.8	19.7	1.3	15.2	0.94
	0-100	0.99	0.45	-0.010	43.3	662	665	114.1	16.4	36.0	16.3	12.8	0.69
	0-200	0.98	0.39	0.055	123.1	769	780	207.1	19.4	97.8	79.2	12.9	0.55
Control	0-30	1.01	0.33	0.000	2.6	361	357	35.9	-	2.4	0.2	19.4	0.93
	0-100	1.01	0.50	0.061	25.7	578	579	111.2	-	20.2	11.0	12.6	0.65
	0-200	0.98	0.40	0.519	57.5	665	681	208.9	-	16.4	85.8	6.3	0.16

490

3.6. Spatial distribution of SOC stocks

491 The AIC (Table 4) of the spatially correlated model were less than that of the spatially
492 uncorrelated model for 2 depths (0-100 cm and 0-200 cm for the agroforestry and the control
493 plots), indicating that spatial correlation should be included in the model of variation. We
494 tested several models of spatial variation and retained the spherical model (Webster and
495 Oliver, 2007). For top soil depth of the two plots (0-30 cm), the AIC of the spatially
496 uncorrelated model was slightly the smallest indicating that the residual variation could be
497 independent once fixed effects had been included in the model. But the difference was very
498 small so we considered the spatially correlated model for the rest of the study. The cross-
499 validation results confirmed the validity of the fitted LMM. The nugget to sill ratio measures
500 the unexplained part of the observed variability. The smallest value was observed for the 0-
501 200 cm depth in the control plot and the higher was observed for the 0-30 cm depth in both
502 plots. When mapping the SOC stocks for three fixed depths with the BLUP in the two plots, a
503 clear pattern can be observed in the agroforestry plot, with high SOC stocks in the tree rows
504 (Fig. 6). The fitted fixed effects indicate that, in average, the SOC stocks were 15 to 20 Mg C
505 ha⁻¹ higher in the tree rows to 30 to 200 cm depth (Table 4). At the opposite, the control plot
506 did not exhibit any spatial pattern.

507

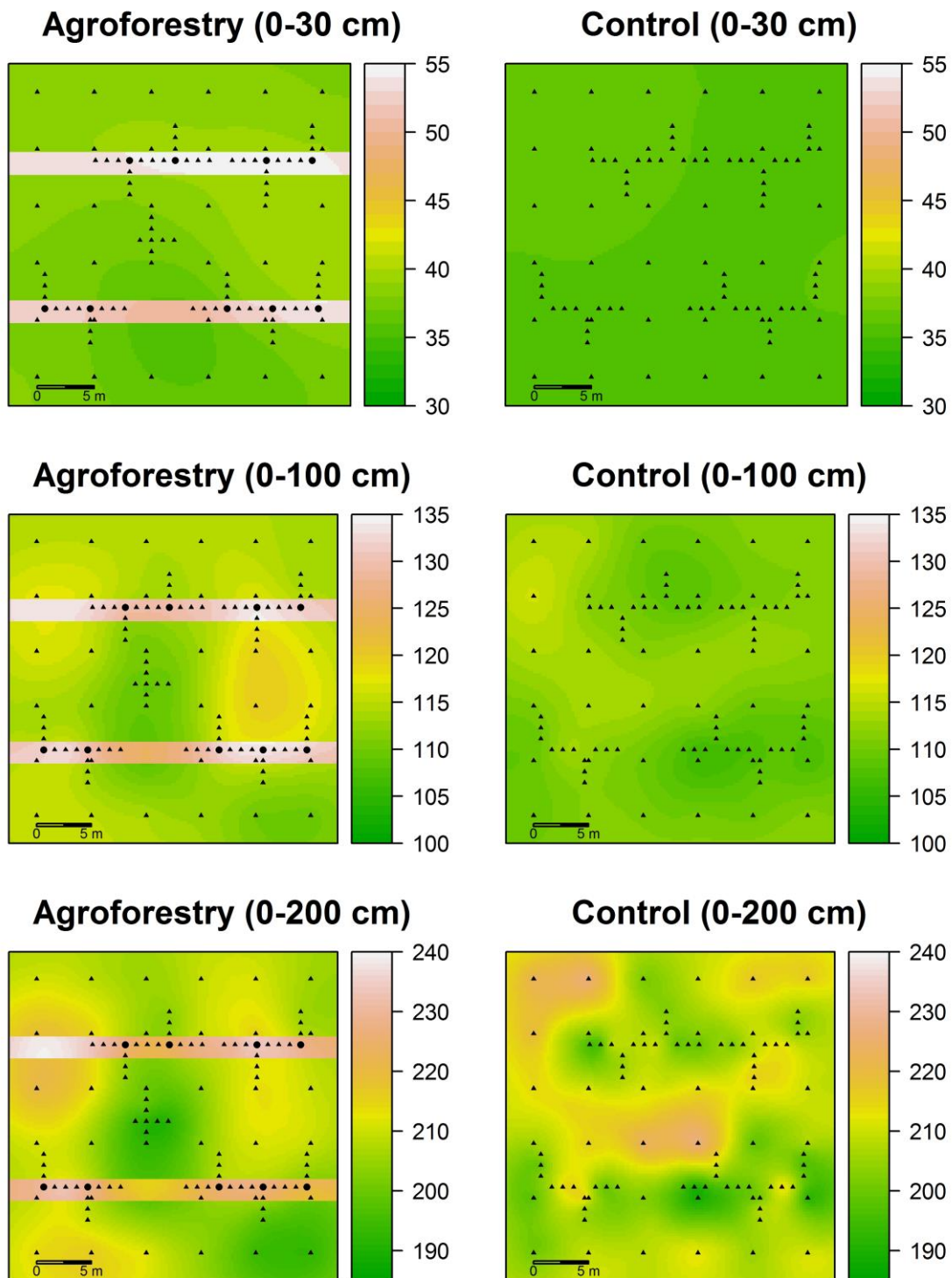
508

509

510

511

512



513

514 Figure 6. Kriged maps of cumulated soil organic carbon stocks (Mg C ha^{-1}) in the
 515 agroforestry and in the control plot.

516

517 *3.7. Organic carbon distribution in soil fractions*

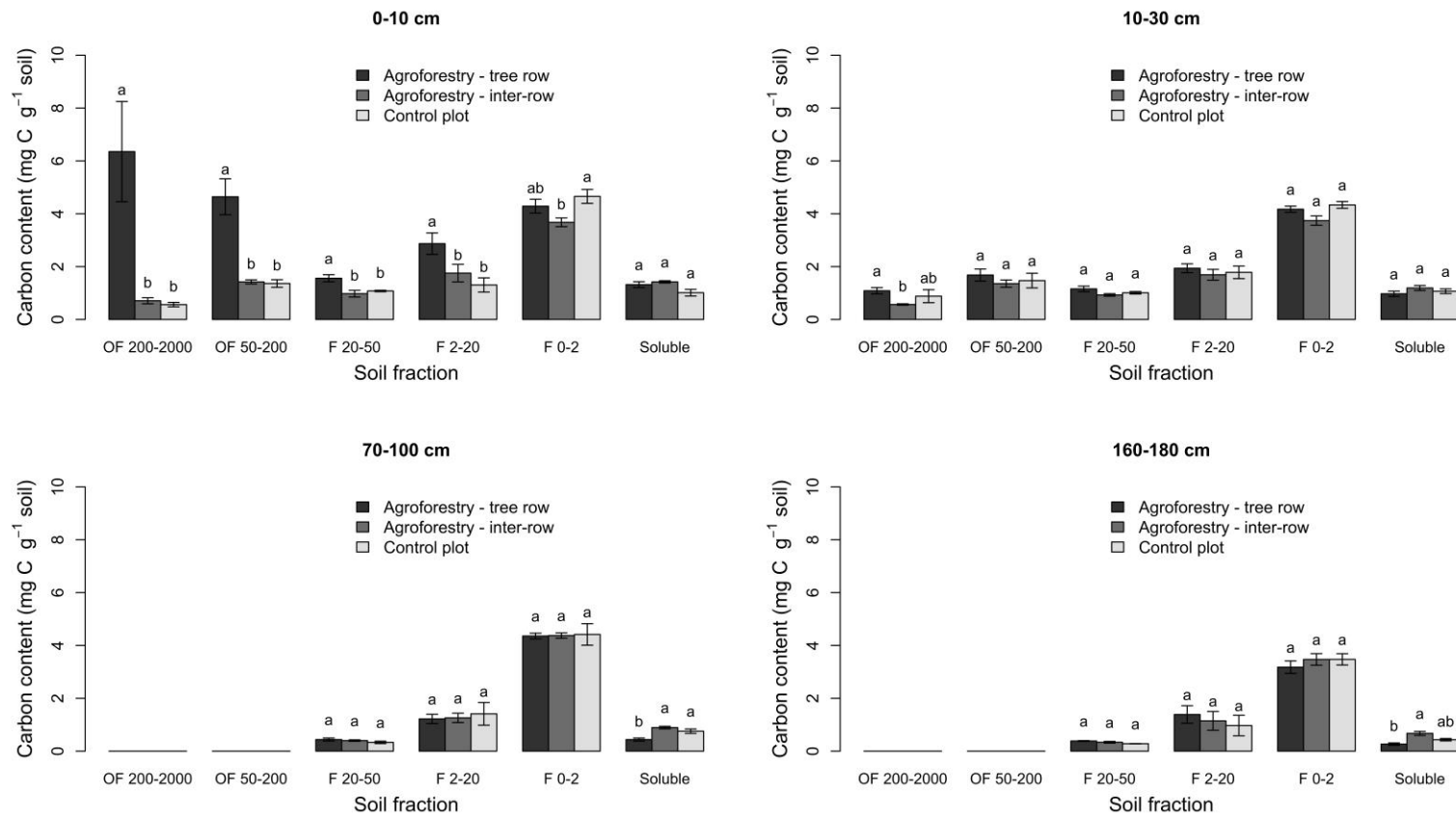
518 An average mass yield of 98% and an average carbon yield of 96% were obtained, showing
519 the quality of the particle size fractionation. Furthermore, the variation between soil texture
520 and soil fractionation was only 5-6% (data not shown). Soil segments used for soil
521 fractionation had similar total SOC concentrations compared to mean SOC concentrations at
522 the same depth (Fig. S2). However, the small differences found between SOC concentrations
523 in the inter row and in the control was not visible with the soil segments used for
524 fractionation.

525 For 0-10 cm depth, the distribution of OC in particle size fractions was strongly modified in
526 the tree rows, with an important increase of C in particulate organic matter (POM) fractions
527 (50-200 μm and 200-2000 μm) compared to the inter-row and to the control (Fig. 7). An
528 increase of C in silt size fractions (2-20 μm and 20-50 μm) of the tree rows compared to the
529 inter row and to the control was also observed. Significantly higher C concentrations in the
530 clay fraction (0-2 μm) were observed in the tree row than in the inter-row (Fig. S3), but it was
531 not the case for the amount of C in the clay fraction per gram of soil (Fig. 7).

532 Similar trends in C distribution in fractions were observed at 10-30 cm depth compared to 0-
533 10 cm, although with much smaller differences (Figs. 7, S3). At deeper depths (70-100 and
534 160-180 cm) there were no differences between the three locations (tree row, inter-row and
535 control) except a lower amount of C in the soluble fraction in the tree row. The potential SOC
536 saturation of particles <20 μm was not reached at any depths (Table 5), and the SOC deficit
537 was high. The saturation capacity was far from being reached, as it amounted 17 to 40% of
538 saturation capacity in the tree rows.

539

540



541

542 Figure 7. Organic carbon contents in each soil fraction (mg C g^{-1} soil). Error bars represent standard errors ($n=6$ in the control, $n=5$ in the inter-
 543 row and in the tree row). OF = Organic fraction, F = organo-mineral fraction. 0-2, 2-20, 20-50, 50-200 and 200-2000 represent particle
 544 size (μm). Means followed by the same letters do not differ significantly at $p=0.017$ (Dunn's test with Bonferroni correction).

545 Table 5. Soil organic carbon saturation of the fractionated soil samples in the agroforestry plot. $SOC_{sat-pot}$, potential SOC saturation ($mg\ C\ g^{-1}$);
 546 SOC_{cur} , current mean SOC concentration of the fine fraction $<20\ \mu m$ ($mg\ C\ g^{-1}$); $SOC_{sat-def}$, SOC saturation deficit ($mg\ C\ g^{-1}$); $SOC_{stor-pot}$,
 547 total amount of the SOC storage potential ($Mg\ C\ ha^{-1}$). Associated errors are standard errors ($n=5$). Values of SOC saturation for deep soil
 548 layers are only indicative.

Depth (cm)	$SOC_{sat-pot}$	SOC_{cur} ($mg\ C\ g^{-1}$)			$SOC_{sat-def}$ ($mg\ C\ g^{-1}$)		$\frac{SOC_{cur}}{SOC_{sat-pot}}$		$SOC_{stor-pot}$
	($mg\ C\ g^{-1}$)	Agroforestry	Tree row	Inter-row	Tree row	Inter-row	Tree row	Inter-row	($Mg\ C\ ha^{-1}$)
0-10	18.0 ± 0.4	7.2 ± 0.3	5.4 ± 0.3	10.3 ± 0.4	13.1 ± 0.4	40%	30%	15.3 ± 0.4	
10-30	18.7 ± 0.4	6.1 ± 0.1	5.4 ± 0.1	12.6 ± 0.3	13.3 ± 0.3	33%	29%	41.8 ± 0.9	
70-100	32.9 ± 0.8	5.6 ± 0.1	5.6 ± 0.1	26.9 ± 0.7	27.6 ± 0.4	17%	17%	140.7 ± 1.9	
160-180	32.0 ± 1.1	4.6 ± 0.2	4.6 ± 0.3	26.8 ± 0.7	28.1 ± 0.9	14%	14%	91.9 ± 2.4	

549 *3.8. Distribution of additional OC in soil fractions*

550 For 0-10 cm depth, the additional OC stored between the tree row and the inter-row was
551 explained at 80% by POM fractions, at 15% by silt size fractions, and at 5% by clay fraction,
552 whereas the additional OC stored between the tree row and the control was explained at 80%
553 by POM and at 20% by silt size fractions (Fig. 7). For 10-30 cm, the additional SOC storage
554 between the tree row and the inter-row was explained at 50% by POM fractions, at 25% by
555 coarse and fine silt fractions, and at 25% by clay fraction (Fig. 7), whereas when comparing
556 the tree row and the control these numbers were of 50% (POM) and 50% (silt).

557

558 **4. Discussion**

559 *4.1. A shallow additional SOC storage*

560 Sampling to 2-m soil depth indicated that the 0-30 cm soil layer contained less than 20% of
561 total SOC stocks to 2-m depth, demonstrating the importance of deeper soil layers for storing
562 SOC (Harper and Tibbett, 2013; Jobbagy and Jackson, 2000). SOC stocks observed in 0-30
563 cm, from 36 to 41 Mg C ha⁻¹, were comparable to reported values for the Mediterranean
564 region, i.e., 25 to 50 Mg C ha⁻¹ (Martin et al., 2011; Muñoz-Rojas et al., 2012). Additional
565 SOC storage in the agroforestry system compared to the agricultural system was mainly
566 observed up to 30 cm soil depth in the inter-row and up to 50 cm in the tree row. A
567 companion study at the same site indicated that 60% of additional OM inputs (leaf litter,
568 aboveground and belowground biomass of the natural vegetation in the tree row, tree fine
569 roots) to 2 m depth in the agroforestry plot compared to the control plot were located in the
570 first 50 cm (unpublished data). Even if 50% of tree fine root density was found between 1 and
571 4 m soil depth (Cardinael et al., 2015), it was also proven at this site (Germon et al.,
572 submitted) and at other sites (Hendrick and Pregitzer, 1996) that the turnover rate of fine roots

573 decreased with increasing depth, resulting in low OM inputs in deep soil layers. Time since
574 the tree planting (18 years) is probably not long enough to detect changes in SOC stocks at
575 deeper soil depths considering low organic inputs below 1 m depth. For 2012, organic C input
576 due to tree fine root mortality was estimated to be less than 150 kg C ha⁻¹ for 100-200 cm soil
577 depth. Below 1.2 m soil depth, delta of cumulated SOC stocks between the agroforestry and
578 the control plot decreased, due to higher SOC concentrations and stocks in the control at these
579 depths. These higher SOC concentrations were linked to higher SOC concentrations in the
580 clay fraction. This difference may be due to pre-experimental soil heterogeneity, the soil in
581 the agroforestry plot may have had a lower level of SOC below 1.2 m depth before tree
582 planting. An initial heterogeneity was also proposed by Upson and Burgess (2013) who found
583 higher SOC stocks at depth in a control plot compared to an agroforestry plot in an
584 experimental site in England . This shows the limit of paired comparisons - or synchronic
585 studies - to evaluate SOC changes after land use change (Junior et al., 2013; Olson et al.,
586 2014), and pleads for long-term diachronic studies in agroforestry systems. An alternative
587 explanation could be a positive priming effect, i.e., the acceleration of native SOC
588 decomposition by the supply of fresh organic carbon (Fontaine et al., 2007, 2004) from the
589 trees. However, this seems highly unlikely since positive priming effect could not explain
590 such a high C loss of about 3.2 Mg C ha⁻¹ between 1.2 and 2.0 m soil depth in 18 years, i.e.,
591 about 180 kg C ha⁻¹ yr⁻¹. Another hypothesis to explain higher SOC stocks below 1.2 m depth
592 in the control plot is a different belowground water regime between the two plots. Water table
593 depth at this site is known to be very variable (between 5 to 7 m). A shallower water table in
594 the agroforestry plot compared to the control plot may promote capillary action, and therefore
595 cause wetting-drying cycles that could enhance SOM decomposition in deep soil layers
596 (Borken and Matzner, 2009).

597

598 *4.2. Tree rows and SOC storage in agroforestry systems*

599 The high SOC stocks observed in tree rows accounted for an important part of SOC stocks of
600 the agroforestry plot even though tree rows only represented 16% of the surface area. In a
601 poplar (*Populus* L.) silvoarable agroforestry experiment in England, Upson and Burgess,
602 (2013) also found that the SOC concentration was greater in the top 40 cm under the tree row
603 (19.6 mg C g⁻¹) in the agroforestry treatment than in the cropped alleys (17 mg C g⁻¹), or the
604 arable control (17.1 mg C g⁻¹). Tree rows are comparable to a natural permanent pasture with
605 trees, given that spontaneous herbaceous vegetation grows and that the soil is not tilled.
606 Conversion of arable lands to permanent grasslands is recognized as an efficient land use for
607 climate change mitigation (Soussana et al., 2004). Grasslands can accumulate SOC at a very
608 high rate. For instance, it was estimated on about 20 years old field experiments that
609 conversion from crop cultivation to pasture stored SOC at a rate of 1.01 Mg C ha⁻¹ yr⁻¹ in 0-30
610 cm (Conant et al., 2001). In our case, SOC accumulation rate in the tree rows was 0.94 ± 0.09
611 Mg C ha⁻¹ yr⁻¹ in 0-30 cm. Management of tree rows could therefore have an important role in
612 improving agroforestry systems in terms of SOC storage. Improved grass species could be
613 sown in the tree rows, as well as shrubs between trees. Further research should focus on this
614 aspect to evaluate benefits in terms of SOC storage and biodiversity for instance.

615

616 *4.3. Homogeneous distribution of SOC stocks in the cropped alley*

617 There was no significant effect of the distance to the trees on SOC stocks at all depths, either
618 in the tree row or in the inter-row. This was also indicated by the maps of the SOC stocks.
619 Tree density was high at this site, and walnuts were about 13 m in height, which is also the
620 distance between two tree rows. This could explain the homogeneous distribution of leaf
621 litterfall observed in the plot (personal observation). In a similar agroforestry system in terms

622 of tree density in Canada, Bambrick et al., (2010) and Peichl et al., (2006) also found no
623 effect of the distance to the trees on SOC stocks to 20 cm depth. They also suggested that the
624 18 m high poplar trees distributed litterfall equally in the crop alleys. Close to the tree rows (1
625 to 2 m distance), the intercrop had a lower yield (15% less in 2012) compared to the middle of
626 the inter-row at the study site (Dufour et al., 2013). On the contrary, tree fine root density was
627 higher close to the tree rows (2.79 t DM ha⁻¹ between 0 and 1.5 m from the tree row in the
628 inter row, and to 4-m soil depth) than in the middle of the inter-rows (1.32 t DM ha⁻¹ between
629 3 and 4.5 m from the tree row in the inter row, and to 4-m soil depth) (Cardinael et al., 2015).
630 Thus, lower carbon inputs from crop residues close to the tree rows may be counterbalanced
631 with higher inputs from tree fine root mortality, explaining homogeneous distribution of SOC
632 stocks within the inter-row (Bambrick et al., 2010; Peichl et al., 2006). In the tree row,
633 homogeneous distribution of SOC stocks may be explained by the short distance between
634 trees and by the presence of abundant herbaceous vegetation.

635

636 *4.4. Agroforestry systems: an efficient land use to improve SOC stocks*

637 Compared to other agroforestry systems having about the same tree density, a lower SOC
638 accumulation rate in 0-30 cm (0.25 Mg C ha⁻¹ yr⁻¹) was observed at our site. Peichl et al.
639 (2006) reported a SOC accumulation rate of 1.04 Mg C ha⁻¹ yr⁻¹ (0-20 cm) in a 13-year old
640 temperate barley (*Hordeum vulgare* L.)-poplar intercropping system (111 trees ha⁻¹). In a 21-
641 year old agroforestry system in Canada where poplars were intercropped with a rotation of
642 wheat (*Triticum aestivum* L.), soybean (*Glycine max* (L.) Merr.) and corn (*Zea mays* L.),
643 Bambrick et al. (2010) estimated a SOC accumulation rate of 0.30 Mg C ha⁻¹ yr⁻¹ (0-20 cm).
644 Our lower accumulation rate may be explained by warmer climate, higher temperatures
645 enhancing OM decomposition (Hamdi et al., 2013). Moreover, valuable hardwood species

646 like walnut trees have a slower growing rate than fast growing species like poplar (Teck and
647 Hilt, 1991), and therefore for a same tree age, the amount of OC inputs (leaf litter, fine roots)
648 to the soil is lower for slow growing species.

649 Together with other climate-smart farming practices (Lipper et al., 2014), alley-cropping
650 agroforestry systems have the potential to enhance SOC stocks and to contribute to climate
651 change mitigation (Nair et al., 2010; Pellerin et al., 2013). No-till farming is a commonly
652 cited agricultural practice supposed to have a positive impact on SOC stocks. But recent meta-
653 analyses showed this practice had no effect on SOC stocks to 40 cm depth (Luo et al., 2010)
654 or a smaller one ($0.23 \text{ Mg C ha}^{-1} \text{ yr}^{-1}$ to 30 cm depth) than previously estimated (Virto et al.,
655 2011). A meta-analysis also revealed that the inclusion of cover crops in cropping systems
656 could accumulate SOC at a rate of $0.32 \pm 0.08 \text{ Mg C ha}^{-1} \text{ yr}^{-1}$ to a depth of 22 cm (Poeplau
657 and Don, 2015). At our site, we found a mean SOC accumulation rate of 0.13 in 0-30 cm in
658 the inter-rows compared to the control. This rate reached $0.25 \text{ Mg C ha}^{-1} \text{ yr}^{-1}$ for the whole
659 agroforestry system. A companion study at this site estimated that the tree aboveground C
660 stock was $117 \pm 21 \text{ kg C tree}^{-1}$ (unpublished data). With 110 trees ha^{-1} , total organic carbon
661 (SOC to 1 m soil depth + aboveground tree C) accumulation rate was $1.11 \pm 0.13 \text{ Mg C ha}^{-1}$
662 yr^{-1} , making agroforestry systems a possible land use to help mitigating climate change (Lal,
663 2004; Lorenz and Lal, 2014).

664

665 *4.5. A long-term SOC storage?*

666 Most of additional SOC in the agroforestry plot compared to the control plot was located in
667 coarse soil fractions (50-200 μm and 200-2000 μm). These soil fractions are assumed to
668 contain labile fractions (Balesdent et al., 1998), that are not stabilized by interaction with
669 clays and thus prone to be decomposed by soil microorganisms. Our site might not be old

670 enough to observe a difference in the fine soil fractions as changes in the clay fractions are
671 often long-term processes (Balesdent, 1996; Balesdent et al., 1988). For example, Takimoto et
672 al., (2008) found in a 35-year-old *Faidherbia albida* parkland in Mali, that the silt + clay soil
673 fraction ($< 53 \mu\text{m}$) was enriched in C at depth compared with treeless systems. But on the
674 other hand, Howlett et al., (2011) did not observe any difference for the same soil fraction in a
675 80 year-old Dehesa cork oak (*Quercus suber* L.) silvopasture, but they found that C storage in
676 the macroaggregate fraction (250–2000 μm) was 68% greater underneath *versus* away from
677 the tree canopy (in 0-25 cm). Several studies have demonstrated that protection of C within
678 the macroaggregate size class was affected by afforestation (Del Galdo et al., 2003; Deneff et
679 al., 2013) and cessation of tillage (Tan et al., 2007). The fractionation method that was used in
680 this study disrupted macroaggregates, and part of this labile fractions could be located within
681 them and therefore be physically protected from decomposition by soil microorganisms (Six
682 et al., 2000). Further work will focus on this aspect in order to estimate the amount of
683 particulate organic matter located in soil aggregates. Calculation of SOC saturation revealed a
684 high deficit of SOC of this soil compared to the theoretical value, suggesting that
685 accumulation of SOC due to the agroforestry system could continue for decades before
686 reaching saturation.

687

688 **5. Conclusion**

689 This study showed the potential of agroforestry systems to increase SOC stocks. However,
690 despite a deep tree rooting system, additional SOC was mainly located in topsoil layers, and
691 in labile organic fractions, making this C storage vulnerable. Tree rows were shown to be a
692 key factor for SOC storage in alley cropping systems. Combining agroforestry systems with
693 no-till or permanent cover systems could be a very efficient way to increase SOC stocks, but
694 more research is needed on this aspect. To fully estimate the impact of agroforestry systems

695 on SOC sequestration, other aspects should be taken into account. For instance, higher SOC
696 stocks in the inter-rows could increase soil fertility and reduce the need for chemical fertilizer,
697 contributing indirectly to a reduction of greenhouse gases emissions; further work should
698 therefore focus on nutrient cycling in these systems.

699

700 **Acknowledgments**

701 This study was financed by the French Environment and Energy Management Agency
702 (ADEME), following a call for proposals as part of the REACCTIF program (Research on
703 Climate Change Mitigation in Agriculture and Forestry). This work was part of the funded
704 project AGRIPSOL (Agroforestry for Soil Protection), coordinated by Agrooof. R. Cardinael
705 was also supported by La Fondation de France. We are very grateful to our colleagues for
706 their help with field and laboratory work and logistics, including Daniel Billiou (UPMC),
707 Emmanuel Bourdon (IRD), Jean-François Bourdoncle (INRA), Lydie Dufour (INRA), Claude
708 Hammecker (IRD), Alain Sellier (INRA) and Manon Villeneuve (IRD). We are also grateful
709 to Valérie Viaud (INRA) for her valuable comments concerning the sampling design and
710 geostatistics, and to Michael Clairotte (INRA) for his help concerning analyses of VNIR
711 spectra. We also thank all students without whom this work would not have been possible,
712 especially Catalina Gomà Pumarino, Guillermo Lobos Norambuena, and Eric Zassi.

713

714

715

716

717 **References**

- 718 Akaike, H., 1974. A new look at the statistical model identification. *IEEE Trans. Automat.*
719 *Contr.* 19, 716–723.
- 720 Albrecht, A., Kandji, S.T., 2003. Carbon sequestration in tropical agroforestry systems. *Agric.*
721 *Ecosyst. Environ.* 99, 15–27.
- 722 Angers, D.A., Arrouays, D., Saby, N.P.A., Walter, C., 2011. Estimating and mapping the
723 carbon saturation deficit of French agricultural topsoils. *Soil Use Manag.* 27, 448–452.
- 724 Balesdent, J., 1996. The significance of organic separates to carbon dynamics and its
725 modelling in some cultivated soils. *Eur. J. Soil Sci.* 47, 485–493.
- 726 Balesdent, J., Balabane, M., 1996. Major contribution of roots to soil carbon storage inferred
727 from maize cultivated soils. *Soil Biol. Biochem.* 28, 1261–1263.
- 728 Balesdent, J., Besnard, E., Arrouays, D., Chenu, C., 1998. The dynamics of carbon in particle-
729 size fractions of soil in a forest-cultivation sequence. *Plant Soil* 201, 49–57.
- 730 Balesdent, J., Wagner, G.H., Mariotti, A., 1988. Soil organic matter turnover in long-term
731 field experiments as revealed by carbon-13 natural abundance. *Soil Sci. Soc. Am. J.* 52,
732 118–124.
- 733 Bambrick, A.D., Whalen, J.K., Bradley, R.L., Cogliastro, A., Gordon, A.M., Olivier, A.,
734 Thevathasan, N. V, 2010. Spatial heterogeneity of soil organic carbon in tree-based
735 intercropping systems in Quebec and Ontario, Canada. *Agrofor. Syst.* 79, 343–353.
- 736 Bausch, J., van der Meer, P., Kanninen, M., 2010. *Ecosystem Goods and Services from*
737 *Plantation Forests.* Earthscan, London, UK.

738 Bellon-Maurel, V., Fernandez-Ahumada, E., Palagos, B., Roger, J.-M., McBratney, A., 2010.
739 Critical review of chemometric indicators commonly used for assessing the quality of the
740 prediction of soil attributes by NIR spectroscopy. *Trends Anal. Chem.* 29, 1073–1081.

741 Bergeron, M., Lacombe, S., Bradley, R.L., Whalen, J., Cogliastro, A., Jutras, M.-F., Arp, P.,
742 2011. Reduced soil nutrient leaching following the establishment of tree-based
743 intercropping systems in eastern Canada. *Agrofor. Syst.* 83, 321–330.

744 Bird, J.A., Torn, M.S., 2006. Fine roots vs. needles: A comparison of ^{13}C and ^{15}N dynamics
745 in a ponderosa pine forest soil. *Biogeochemistry* 79, 361–382.

746 Borken, W., Matzner, E., 2009. Reappraisal of drying and wetting effects on C and N
747 mineralization and fluxes in soils. *Glob. Chang. Biol.* 15, 808–824.

748 Brown, D.J., Shepherd, K.D., Walsh, M.G., Dewayne Mays, M., Reinsch, T.G., 2006. Global
749 soil characterization with VNIR diffuse reflectance spectroscopy. *Geoderma* 132, 273–
750 290.

751 Cardinael, R., Mao, Z., Prieto, I., Stokes, A., Dupraz, C., Jourdan, C., 2015. Competition with
752 winter crops induces deeper rooting of walnut trees in a Mediterranean alley cropping
753 agroforestry system. *Plant Soil* 391, 219–235.

754 Chang, C., Laird, D.A., Mausbach, M.J., Hurburgh, C.R., 2001. Near-Infrared Reflectance
755 Spectroscopy–Principal Components Regression Analyses of Soil Properties. *Soil Sci.*
756 *Soc. Am. J.* 65, 480–490.

757 Chenu, C., Plante, A.F., 2006. Clay-sized organo-mineral complexes in a cultivation
758 chronosequence: revisiting the concept of the “primary organo-mineral complex.” *Eur. J.*
759 *Soil Sci.* 57, 596–607.

760 Clough, Y., Barkmann, J., Juhbandt, J., Kessler, M., Wanger, T.C., Anshary, A., Buchori, D.,
761 Cicuzza, D., Darras, K., Putra, D.D., Erasmi, S., Pitopang, R., Schmidt, C., Schulze,
762 C.H., Seidel, D., Steffan-Dewenter, I., Stenchly, K., Vidal, S., Weist, M., Wielgoss,
763 A.C., Tschardtke, T., 2011. Combining high biodiversity with high yields in tropical
764 agroforests. *PNAS* 108, 8311–6.

765 Conant, R.T., Paustian, K., Elliott, E.T., 2001. Grassland management and conversion into
766 grassland: effects on soil carbon. *Ecol. Appl.* 11, 343–355.

767 Conant, R.T., Ryan, M.G., Ågren, G.I., Birge, H.E., Davidson, E.A., Eliasson, P.E., Evans,
768 S.E., Frey, S.D., Giardina, C.P., Hopkins, F.M., Hyvönen, R., Kirschbaum, M.U.F.,
769 Lavalley, J.M., Leifeld, J., Parton, W.J., Megan Steinweg, J., Wallenstein, M.D., Martin
770 Wetterstedt, J.Å., Bradford, M.A., 2011. Temperature and soil organic matter
771 decomposition rates - synthesis of current knowledge and a way forward. *Glob. Chang.*
772 *Biol.* 17, 3392–3404.

773 Del Galdo, I., Six, J., Peressotti, A., Cotrufo, M.F., 2003. Assessing the impact of land-use
774 change on soil C sequestration in agricultural soils by means of organic matter
775 fractionation and stable C isotopes. *Glob. Chang. Biol.* 9, 1204–1213.

776 Denef, K., Galdo, I. Del, Venturi, A., Cotrufo, M.F., 2013. Assessment of Soil C and N
777 Stocks and Fractions across 11 European Soils under Varying Land Uses. *Open J. Soil*
778 *Sci.* 3, 297–313.

779 Dufour, L., Metay, A., Talbot, G., Dupraz, C., 2013. Assessing Light Competition for Cereal
780 Production in Temperate Agroforestry Systems using Experimentation and Crop
781 Modelling. *J. Agron. Crop Sci.* 199, 217–227.

- 782 Dunn, O.J., 1964. Multiple comparisons using rank sums. *Technometrics* 6, 241–252.
- 783 Ellert, B.H., Bettany, J.R., 1995. Calculation of organic matter and nutrients stored in soils
784 under contrasting management regimes. *Can. J. Soil Sci.* 75, 529–538.
- 785 Ellert, B.H., Janzen, H.H., Entz, T., 2002. Assessment of a Method to Measure Temporal
786 Change in Soil Carbon Storage. *Soil Sci. Soc. Am. J.* 66, 1687–1695.
- 787 Fontaine, S., Bardoux, G., Abbadie, L., Mariotti, A., 2004. Carbon input to soil may decrease
788 soil carbon content. *Ecol. Lett.* 7, 314–320.
- 789 Fontaine, S., Barot, S., Barré, P., Bdioui, N., Mary, B., Rumpel, C., 2007. Stability of organic
790 carbon in deep soil layers controlled by fresh carbon supply. *Nature* 450, 277–281.
- 791 Gale, W.J., Cambardella, C.A., Bailey, T.B., 2000. Root-Derived Carbon and the Formation
792 and Stabilization of Aggregates. *Soil Sci. Soc. Am. J.* 64, 201.
- 793 Gavinelli, E., Feller, C., Larré-Larrouy, M., Bacye, B., Djegui, N., Nzila, J. de D., 1995. A
794 routine method to study soil organic matter by particle-size fractionation: examples for
795 tropical soils. *Commun. Soil Sci. Plant Anal.* 26, 1749–1760.
- 796 Germon, A., Cardinael, R., Prieto, I., Mao, Z., Kim, J.H., Stokes, A., Dupraz, C., Laclau, J.-
797 P., Jourdan, C. Unexpected phenology and lifespan of shallow and deep fine roots of
798 walnut trees grown in a Mediterranean agroforestry system (submitted).
- 799 Gras, J.-P., Barthès, B.G., Mahaut, B., Trupin, S., 2014. Best practices for obtaining and
800 processing field visible and near infrared (VNIR) spectra of topsoils. *Geoderma* 214-215,
801 126–134.

802 Haile, S.G., Nair, V.D., Nair, P.K.R., 2010. Contribution of trees to carbon storage in soils of
803 silvopastoral systems in Florida, USA. *Glob. Chang. Biol.* 16, 427–438.

804 Hamdi, S., Moyano, F., Sall, S., Bernoux, M., Chevallier, T., 2013. Synthesis analysis of the
805 temperature sensitivity of soil respiration from laboratory studies in relation to
806 incubation methods and soil conditions. *Soil Biol. Biochem.* 58, 115–126.

807 Harper, R.J., Tibbett, M., 2013. The hidden organic carbon in deep mineral soils. *Plant Soil*
808 368, 641–648.

809 Harris, D., Horwath, W.R., Van Kessel, C., 2001. Acid fumigation of soils to remove
810 carbonates prior to total organic carbon or carbon-13 isotopic analysis. *Soil Sci. Soc.*
811 *Am. J.* 65, 1853–1856.

812 Hassink, J., 1997. The capacity of soils to preserve organic C and N by their association with
813 clay and silt particles. *Plant Soil* 191, 77–87.

814 Hothorn, T., Bretz, F., Westfall, P., 2008. Simultaneous Inference in General Parametric
815 Models. *Biometrical J.* 50, 346–363.

816 Howlett, D.S., Moreno, G., Mosquera Losada, M.R., Nair, P.K.R., Nair, V.D., 2011. Soil
817 carbon storage as influenced by tree cover in the Dehesa cork oak silvopasture of central-
818 western Spain. *J. Environ. Monit.* 13, 1897–904.

819 IUSS Working Group WRB, 2007. World Reference Base for Soil Resources 2006, first
820 update 2007. World Soil Resources Reports No. 103. FAO, Rome.

821 Jobbagy, E.G., Jackson, R.B., 2000. The vertical distribution of soil organic carbon and its
822 relation to climate and vegetation. *Ecol. Appl.* 10, 423–436.

823 Jordan, C.F., 2004. Organic farming and agroforestry: Alleycropping for mulch production
824 for organic farms of southeastern United States. *Agrofor. Syst.* 61-62, 79–90.

825 Junior, C.C., Corbeels, M., Bernoux, M., Piccolo, M.C., Neto, M.S., Feigl, B.J., Cerri, C.E.P.,
826 Cerri, C.C., Scopel, E., Lal, R., 2013. Assessing soil carbon storage rates under no-
827 tillage: Comparing the synchronic and diachronic approaches. *Soil Tillage Res.* 134,
828 207–212.

829 Kennard, R.W., Stone, L.A., 1969. Computer aided design of experiments. *Technometrics* 11,
830 137–148.

831 Kruskal, W.H., Wallis, W.A., 1952. Use of Ranks in One-Criterion Variance Analysis. *J. Am.*
832 *Stat. Assoc.* 47, 583–621.

833 Lal, R., 2004. Soil carbon sequestration impacts on global climate change and food security.
834 *Science* (80-.). 304, 1623–7.

835 Lal, R., 2004. Soil carbon sequestration to mitigate climate change. *Geoderma* 123, 1–22.

836 Lark, R.M., Cullis, B.R., Welham, S.J., 2006. On spatial prediction of soil properties in the
837 presence of a spatial trend: the empirical best linear unbiased predictor (E-BLUP) with
838 REML. *Eur. J. Soil Sci.* 57, 787–799.

839 Lipper, L., Thornton, P., Campbell, B.M., Baedeker, T., Braimoh, A., Bwalya, M., Caron, P.,
840 Cattaneo, A., Garrity, D., Henry, K., Hottle, R., Jackson, L., Jarvis, A., Kossam, F.,
841 Mann, W., McCarthy, N., Meybeck, A., Neufeldt, H., Remington, T., Sen, P.T., Sessa,
842 R., Shula, R., Tibu, A., Torquebiau, E.F., 2014. Climate-smart agriculture for food
843 security. *Nat. Clim. Chang.* 4, 1068–1071.

844 Lorenz, K., Lal, R., 2014. Soil organic carbon sequestration in agroforestry systems. A
845 review. *Agron. Sustain. Dev.* 34, 443–454.

846 Luo, Z., Wang, E., Sun, O.J., 2010. Can no-tillage stimulate carbon sequestration in
847 agricultural soils? A meta-analysis of paired experiments. *Agric. Ecosyst. Environ.* 139,
848 224–231.

849 Martens, H., Naes, T., 1989. *Multivariate calibration*. John Wiley & Sons, Ltd, Chichester.

850 Martin, M.P., Wattenbach, M., Smith, P., Meersmans, J., Jolivet, C., Boullonne, L., Arrouays,
851 D., 2011. Spatial distribution of soil organic carbon stocks in France. *Biogeosciences* 8,
852 1053–1065.

853 Millennium Ecosystem Assessment, 2005. *Ecosystems and Human Well-being: Synthesis*.
854 Island Press, Washington, DC.

855 Mulia, R., Dupraz, C., 2006. Unusual fine root distributions of two deciduous tree species in
856 southern France: What consequences for modelling of tree root dynamics? *Plant Soil*
857 281, 71–85.

858 Muñoz-Rojas, M., Jordán, A., Zavala, L.M., De la Rosa, D., Abd-Elmabod, S.K., Anaya-
859 Romero, M., 2012. Organic carbon stocks in Mediterranean soil types under different
860 land uses (Southern Spain). *Solid Earth* 3, 375–386.

861 Nair, P.K.R., 2012. Carbon sequestration studies in agroforestry systems: a reality-check.
862 *Agrofor. Syst.* 86, 243–253.

863 Nair, P.K.R., Nair, V.D., Kumar, B.M., Showalter, J.M., 2010. Carbon sequestration in
864 agroforestry systems, in: *Advances in Agronomy*. pp. 237–307.

865 Oades, J., 1995. An overview of processes affecting the cycling of organic carbon in soils, in:
866 Zepp, R.G., Sonntag, C. (Eds.), Role of Non-Living Organic Matter in the Earth's
867 Carbon Cycle. John Wiley, pp. 293–303.

868 Oelbermann, M., Voroney, R.P., 2007. Carbon and nitrogen in a temperate agroforestry
869 system: Using stable isotopes as a tool to understand soil dynamics. *Ecol. Eng.* 29, 342–
870 349.

871 Oelbermann, M., Voroney, R.P., Gordon, A.M., 2004. Carbon sequestration in tropical and
872 temperate agroforestry systems: a review with examples from Costa Rica and southern
873 Canada. *Agric. Ecosyst. Environ.* 104, 359–377.

874 Olson, K.R., Al-Kaisi, M., Lal, R., Lowery, B., 2014. Examining the paired comparison
875 method approach for determining soil organic carbon sequestration rates. *J. Soil Water*
876 *Conserv.* 69, 193A–197A.

877 Pandey, D.N., 2002. Carbon sequestration in agroforestry systems. *Clim. Policy* 2, 367–377.

878 Peichl, M., Thevathasan, N. V, Gordon, A.M., Huss, J., Abohassan, R.A., 2006. Carbon
879 sequestration potentials in temperate tree-based intercropping systems, southern Ontario,
880 Canada. *Agrofor. Syst.* 66, 243–257.

881 Pellerin, S., Bamière, L., Angers, D., Béline, F., Benoît, M., Butault, J.P., Chenu, C.,
882 Colnenne-David, C., De Cara, S., Delame, N., Doreau, M., Dupraz, P., Faverdin, P.,
883 Garcia-Launay, F., Hassouna, M., Hénault, C., Jeuffroy, M., Klumpp, K., Metay, A.,
884 Moran, D., Recous, S., Samson, E., Savini, I., Pardon, L., 2013. How can French
885 agriculture contribute to reducing greenhouse gas emissions? Abatement potential and
886 cost of ten technical measures. Synopsis of the study report, INRA (France).

887 Philippot, L., Čuhel, J., Saby, N.P.A., Chèneby, D., Chroňáková, A., Bru, D., Arrouays, D.,
888 Martin-Laurent, F., Šimek, M., 2009. Mapping field-scale spatial patterns of size and
889 activity of the denitrifier community. *Environ. Microbiol.* 11, 1518–1526.

890 Pinheiro, J., Bates, D., DebRoy, S., Sarkar, D., R Development Core Team, 2013. nlme:
891 Linear and Nonlinear Mixed Effects Models. R package version 3.1-111.

892 Pinheiro, J.C., Bates, D.M., 2000. *Mixed-Effects Models in S and S-PLUS*. Springer Science
893 & Business Media.

894 Poeplau, C., Don, A., 2015. Carbon sequestration in agricultural soils via cultivation of cover
895 crops – A meta-analysis. *Agric. Ecosyst. Environ.* 200, 33–41.

896 Power, A.G., 2010. Ecosystem services and agriculture: tradeoffs and synergies. *Philos.*
897 *Trans. R. Soc. Lond. B. Biol. Sci.* 365, 2959–2971.

898 Profft, I., Mund, M., Weber, G.-E., Weller, E., Schulze, E.-D., 2009. Forest management and
899 carbon sequestration in wood products. *Eur. J. For. Res.* 128, 399–413.

900 Puget, P., Chenu, C., Balesdent, J., 2000. Dynamics of soil organic matter associated with
901 particle-size fractions of water-stable aggregates. *Eur. J. Soil Sci.* 51, 595–605.

902 R Development Core Team, 2013. *R: A language and environment for statistical computing*.

903 Rasse, D.P., Rumpel, C., Dignac, M.F., 2005. Is soil carbon mostly root carbon? Mechanisms
904 for a specific stabilisation. *Plant Soil* 269, 341–356.

905 Rhoades, C.C., 1997. Single-tree influences on soil properties in agroforestry: lessons from
906 natural forest and savanna ecosystems. *Agrofor. Syst.* 35, 71–94.

907 Ribeiro, P.J., Diggle, P.J., 2001. geoR: A package for geostatistical analysis. R-News 1, 15–
908 18.

909 Schroth, G., da Fonseca, G.A.B., Harvey, C.A., Gascon, C., Vasconcelos, H.L., Izac, A.-
910 M.N., 2004. Agroforestry and biodiversity conservation in tropical landscapes. Island
911 Press, Washington, DC.

912 Sharrow, S.H., Ismail, S., 2004. Carbon and nitrogen storage in agroforests, tree plantations,
913 and pastures in western Oregon, USA. Agrofor. Syst. 60, 123–130.

914 Six, J., Elliott, E.T., Paustian, K., 2000. Soil macroaggregate turnover and microaggregate
915 formation: a mechanism for C sequestration under no-tillage agriculture. Soil Biol.
916 Biochem. 32, 2099–2103.

917 Six, J., Elliott, E.T., Paustian, K., Doran, J.W., 1998. Aggregation and soil organic matter
918 accumulation in cultivated and native grassland soils. Soil Sci. Soc. Am. J. 62, 1367–
919 1377.

920 Somarriba, E., 1992. Revisiting the past: an essay on agroforestry definition. Agrofor. Syst.
921 19, 233–240.

922 Somarriba, E., Cerda, R., Orozco, L., Cifuentes, M., Dávila, H., Espin, T., Mavisoy, H.,
923 Ávila, G., Alvarado, E., Poveda, V., Astorga, C., Say, E., Deheuvels, O., 2013. Carbon
924 stocks and cocoa yields in agroforestry systems of Central America. Agric. Ecosyst.
925 Environ. 173, 46–57.

926 Soussana, J.-F., Loiseau, P., Vuichard, N., Ceschia, E., Balesdent, J., Chevallier, T., Arrouays,
927 D., 2004. Carbon cycling and sequestration opportunities in temperate grasslands. Soil
928 Use Manag. 20, 219–230.

929 Stavi, I., Lal, R., 2013. Agroforestry and biochar to offset climate change: a review. *Agron.*
930 *Sustain. Dev.* 33, 81–96.

931 Stevens, A., Nocita, M., Tóth, G., Montanarella, L., van Wesemael, B., 2013. Prediction of
932 Soil Organic Carbon at the European Scale by Visible and Near InfraRed Reflectance
933 Spectroscopy. *PLoS One* 8, 1–13.

934 Takimoto, A., Nair, V.D., Nair, P.K.R., 2008. Contribution of trees to soil carbon
935 sequestration under agroforestry systems in the West African Sahel. *Agrofor. Syst.* 76,
936 11–25.

937 Tan, Z., Lal, R., Owens, L., Izaurrealde, R., 2007. Distribution of light and heavy fractions of
938 soil organic carbon as related to land use and tillage practice. *Soil Tillage Res.* 92, 53–
939 59.

940 Teck, R.M., Hilt, D.E., 1991. Individual-Tree Diameter Growth Model for the Northeastern
941 United States. Res. Pap. NE-649. Radnor, PA: US. Department of Agriculture, Forest
942 Service, Northeastern Forest Experiment Station. 11 p.

943 Torquebiau, E.F., 2000. A renewed perspective on agroforestry concepts and classification.
944 *Life Sci.* 323, 1009–1017.

945 Tully, K.L., Lawrence, D., Scanlon, T.M., 2012. More trees less loss: Nitrogen leaching
946 losses decrease with increasing biomass in coffee agroforests. *Agric. Ecosyst. Environ.*
947 161, 137–144.

948 Upson, M.A., Burgess, P.J., 2013. Soil organic carbon and root distribution in a temperate
949 arable agroforestry system. *Plant Soil* 373, 43–58.

950 Varah, A., Jones, H., Smith, J., Potts, S.G., 2013. Enhanced biodiversity and pollination in
951 UK agroforestry systems. *J. Sci. Food Agric.* 93, 2073–5.

952 Verchot, L. V., Noordwijk, M., Kandji, S., Tomich, T., Ong, C., Albrecht, A., Mackensen, J.,
953 Bantilan, C., Anupama, K. V., Palm, C., 2007. Climate change: linking adaptation and
954 mitigation through agroforestry. *Mitig. Adapt. Strateg. Glob. Chang.* 12, 901–918.

955 Villanneau, E.J., Saby, N.P.A., Marchant, B.P., Jolivet, C.C., Boulonne, L., Caria, G.,
956 Barriuso, E., Bispo, A., Briand, O., Arrouays, D., 2011. Which persistent organic
957 pollutants can we map in soil using a large spacing systematic soil monitoring design? A
958 case study in Northern France. *Sci. Total Environ.* 409, 3719–3731.

959 Virto, I., Barré, P., Burlot, A., Chenu, C., 2011. Carbon input differences as the main factor
960 explaining the variability in soil organic C storage in no-tilled compared to inversion
961 tilled agrosystems. *Biogeochemistry* 108, 17–26.

962 Von Lützow, M., Kögel-Knabner, I., Ekschmitt, K., Flessa, H., Guggenberger, G., Matzner,
963 E., Marschner, B., 2007. SOM fractionation methods: Relevance to functional pools and
964 to stabilization mechanisms. *Soil Biol. Biochem.* 39, 2183–2207.

965 Webster, R., McBratney, A.B., 1989. On the Akaike Information Criterion for choosing
966 models for variograms of soil properties. *J. Soil Sci.* 40, 493–496.

967 Webster, R., Oliver, M.A., 2007. *Geostatistics for Environmental Scientists*.

968 Wiesmeier, M., Hübner, R., Spörlein, P., Geuß, U., Hangen, E., Reischl, A., Schilling, B., von
969 Lützow, M., Kögel-Knabner, I., 2014. Carbon sequestration potential of soils in
970 southeast Germany derived from stable soil organic carbon saturation. *Glob. Chang.*
971 *Biol.* 20, 653–665.

972 Young, A., 1997. Agroforestry for Soil Management, Second. ed. CAB International,
973 Wallingford, UK.

974

975

976

977

978

979

980

981

982

983

984

985

986

987

988

989

990

991 **Supplementary materials**

992 Table S1. Soil organic carbon stocks (Mg C ha⁻¹) and SOC accumulation rates (kg C ha⁻¹ yr⁻¹)
 993 without the equivalent soil mass (ESM) correction. Associated errors are standard errors (100
 994 replicates for the agroforestry plot, 93 for the control plot).

Soil depth (cm)	Cumulated SOC stocks (Mg C ha ⁻¹)		Δ SOC stocks (Mg C ha ⁻¹)	SOC accumulation rates (kg C ha ⁻¹ yr ⁻¹)
	Agroforestry	Control	Δ (Agroforestry – Control)	Agroforestry vs Control
0-10	13.9 ± 0.3	13.2 ± 0.1	0.7 ± 0.4	41 ± 20
0-30	44.5 ± 0.5	41.9 ± 0.2	2.5 ± 0.6	139 ± 32
0-50	67.9 ± 0.7	65.5 ± 0.4	2.5 ± 0.8	137 ± 42
0-70	88.8 ± 0.7	86.3 ± 0.4	2.6 ± 0.8	143 ± 46
0-100	121.2 ± 0.7	118.0 ± 0.5	3.1 ± 0.9	173 ± 54
0-120	140.9 ± 0.8	138.4 ± 0.6	2.5 ± 1.0	138 ± 56
0-140	161.4 ± 0.8	159.4 ± 0.6	1.9 ± 1.0	106 ± 58
0-160	181.5 ± 0.8	180.5 ± 0.6	0.9 ± 1.0	53 ± 60
0-180	199.5 ± 0.9	199.3 ± 0.6	0.2 ± 1.1	11 ± 60
0-200	214.6 ± 0.9	214.5 ± 0.6	0.1 ± 1.1	7 ± 62

995

996

997

998

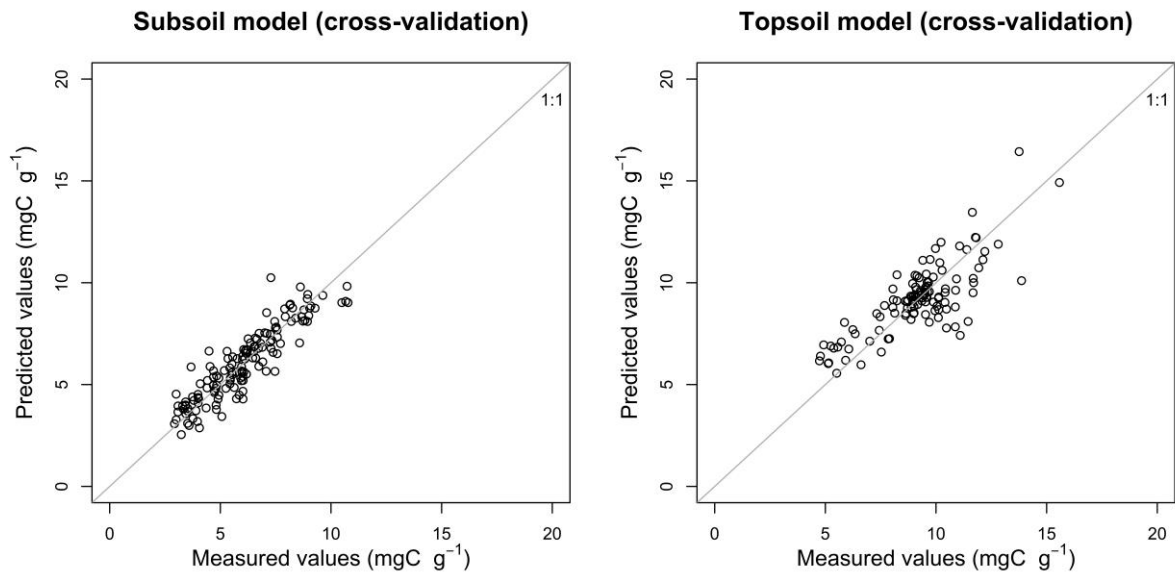
999

1000

1001

1002

1003



1004

1005 Figure S1. Measured and cross-validation predicted values of soil organic carbon
1006 concentrations for the topsoil and subsoil models.

1007

1008

1009

1010

1011

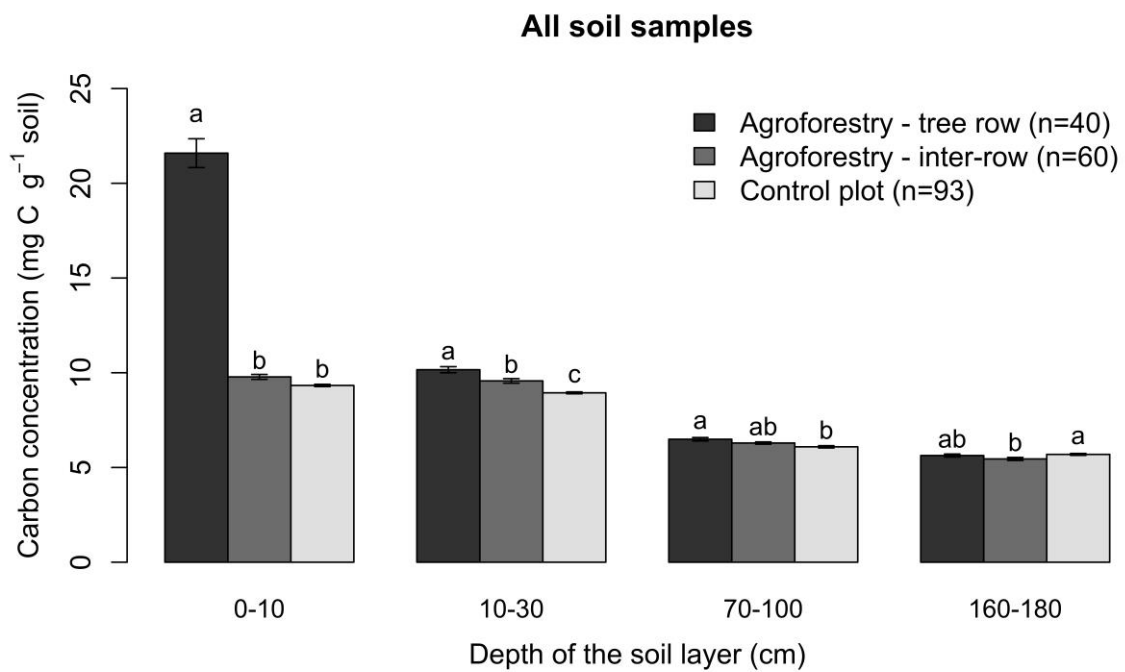
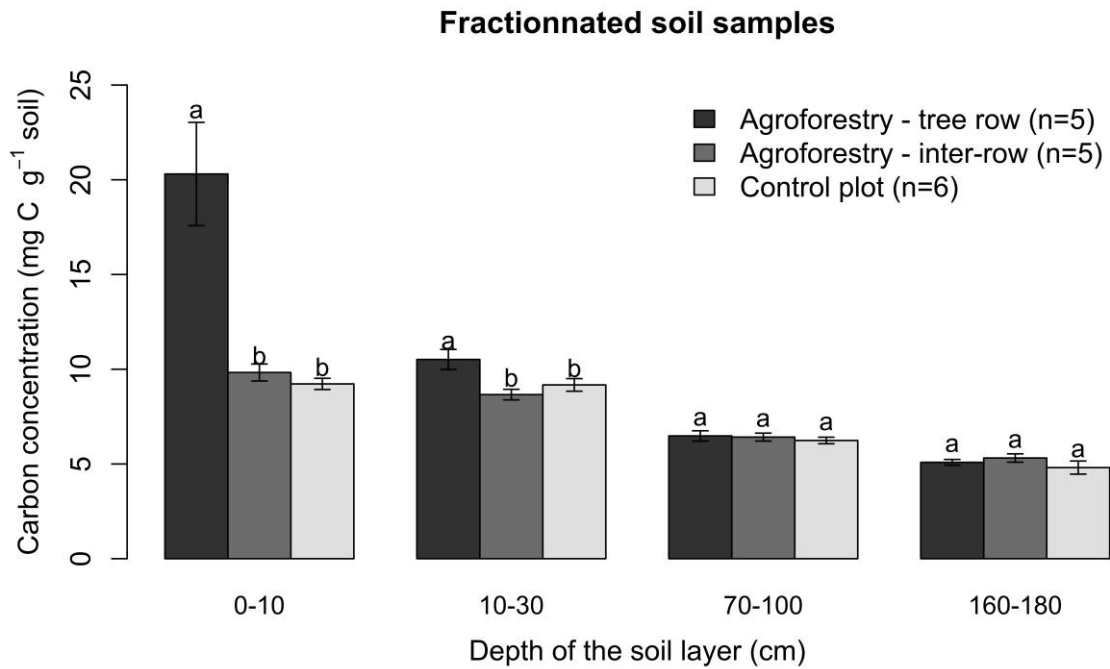
1012

1013

1014

1015

1016



1017

1018 Figure S2. Carbon concentration of bulk fractionated samples. Error bars represent standard
 1019 errors (n=6 in the control, n=5 in the inter-row and in the tree row).

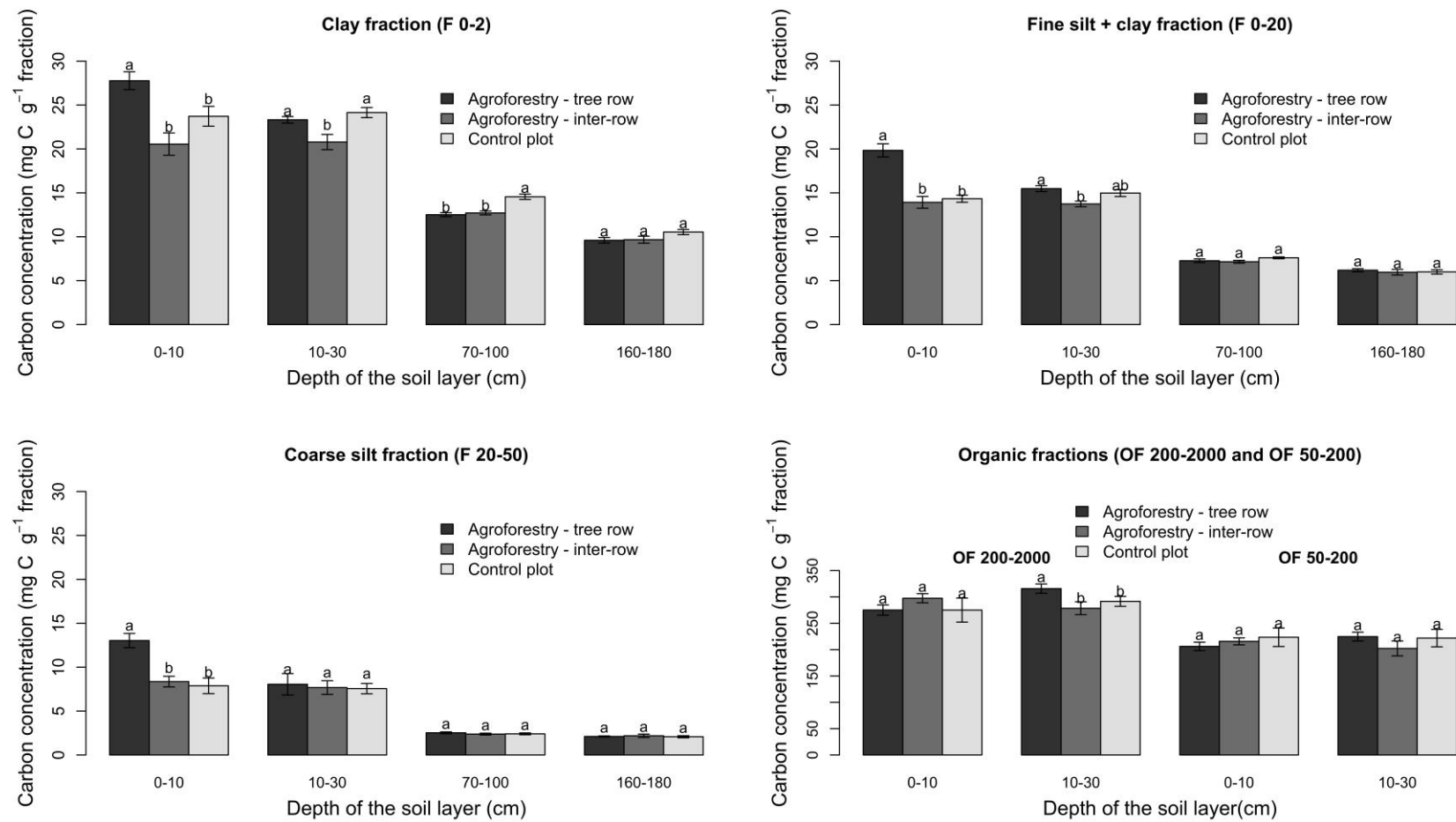


Figure S3. Carbon concentration of each soil fraction. Error bars represent standard errors (n=6 in the control, n=5 in the inter-row and in the tree row). OF = Organic fraction, F = organo-mineral fraction. Means followed by the same letters do not differ significantly at p=0.017 (Dunn's test with Bonferroni correction).